Faculteit der Natuurwetenschappen, Wiskunde en Informatica
MSc Physics and Astronomy
Advanced Matter and Energy Physics

Triplet Energy Transfer in Singlet Fission Silicon Solar Cells

by

Joris Bodin
10773991

July 2019
60 ECTS
September 2018 - July 2019

Supervisors:
dr. Bruno Ehrler
prof. dr. Albert Polman

Abstract

Singlet fission enhanced solar cells have great potential in overcoming the fundamental efficiency limits applying to conventional silicon solar cells. By efficient downconversion in a singlet fission material, one absorbed photon can form two excited triplet excitons via singlet fission. Subsequently, the two triplet excitons can transfer their energy into a low-bandgap absorber, where they can be efficiently extracted. The main challenge in realizing efficient singlet fission enhanced solar cells is efficient energy transfer from the singlet fission material to the low band-gap semiconductor, which has not been shown yet except very recently in photovoltaic devices. This thesis aims to provide experimental evidence for the existence of such energy transfer by magnetic field-dependent photocurrent measurements and quantum efficiency measurements in a hybrid solar cell, consisting of a singlet fission material add-on layer on top of a conventional back-contacted silicon solar cell. Magnetic field-dependent photocurrent measurements based on Johnson-Merrifield theory initially show that the energy of the singlet excitons transfers to the silicon solar cell by means of photon transfer. However, after an aging time that allows native silicon oxide to grow on the silicon solar cell surface, triplet energy transfer is observed. Quantum efficiency measurements show that the efficiency of this triplet energy transfer is below 5%.

Acknowledgements

I would like to express many thanks to everybody who helped me finish this thesis. First of all, Benjamin for all of his fantastic help during my project here at AMOLF and for always making time to answer all my questions or just to look for stuff with me. Secondly, I would like to thank Bruno for being a great supervisor and for giving me the opportunity to do my master project in the Hybrid Solar Cells group. From this fantastic group of people, I would also like to thank Lucie, Moritz and Christian for helping with lab equipment from time to time and all of the group members for the great working atmosphere and their kindness in general. I would also like to thank Albert, for being the examiner of this work. Furthermore, I would like to thank Stefan and ECN for providing some wonderful silicon solar cells for our experiments and Alyssa for doing XPS measurements and organically passivating our devices. Finally, I would like to thank my family and my friends for their mental support.

Contents

1 Introduction

1.1 Energy transition from fossil to PV

The Paris Agreement, which set the goal to prevent the earth from warming up more than 1.5^o Celsius, entered into force in 2016 and has since been ratified by as many as 185 of 197 parties in the United Nations Framework Convention on Climate Change.[1] To achieve this goal, the energy sector has been faced with the challenge to make the transition from fossil-based fuels to renewable energy sources, such are wind power, hydropower and solar energy. Since solar energy is by far the most abundant renewable energy resource, this transition means for the largest part that the production of electricity should be done by conversing solar energy into electric energy, rather than by the conversion of chemical energy in conventional fossil fuel-based power plants. The conversion of solar energy into electricity is easiest done using photovoltaic cells, where incoming sunlight is directly used in a semiconductor material to excite charge carriers (electrons and holes) to higher-energy states. The generated charge carriers are subsequently separated, resulting in an operating voltage that is able to deliver continuous power under illumination. Extensive research by the solar cell industry has led to an exponential growth of installed photovoltaic (PV) capacity over the last 50 years, resulting in a corresponding exponential decrease of solar cell module prices. This trend is predicted to continue for the next decade.[2]

However, solar cell module prices are not the only costs that constitute the total cost of new solar energy installations. Balance of system (BOS) costs, such as labor, the cost of structural and electrical components, the inverter and potential land acquisition costs and taxes, will be a rising fraction of the total costs of newly installed solar systems,[3] as is shown in figure 1.1. Therefore, to further decrease the cost of electricity generated by solar modules, focus should be on increasing their power conversion efficiency.

The power conversion efficiency of solar cells is limited by various fundamental thermodynamic principles. This was first described by Shockley and Queisser[4] and is visualized in figure 1.2 and described below. For ideal silicon devices, the maximum achievable power conversion efficiency has been calculated to be 29.4%.[5] With record laboratory efficiency's as high as 26.7% being reported[6] for silicon, little room is left for efficiency improvement of these solar cells.[7] Therefore, innovative approaches to circumvent the limits posed by Shockley

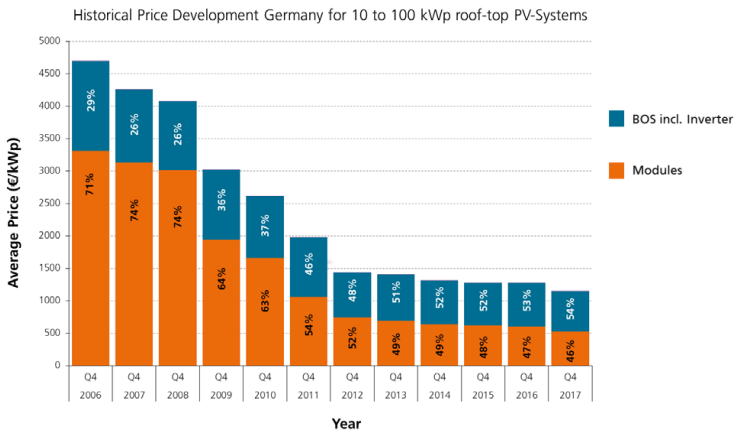

Figure 1.1: Historic price development of roof-top PV-systems in Germany over the last decade.[3] A spectacular decrease in price is visible, mainly caused by decrease of module prices as a result of lower manufacturing costs. A consequence of this is that the balance of system costs have an ever increasing share in the total cost of PV-systems.

and Queisser should be explored. In order to do this, we first look at the fundamental process causing the largest energy loss in single-junction solar cells: spectral losses.

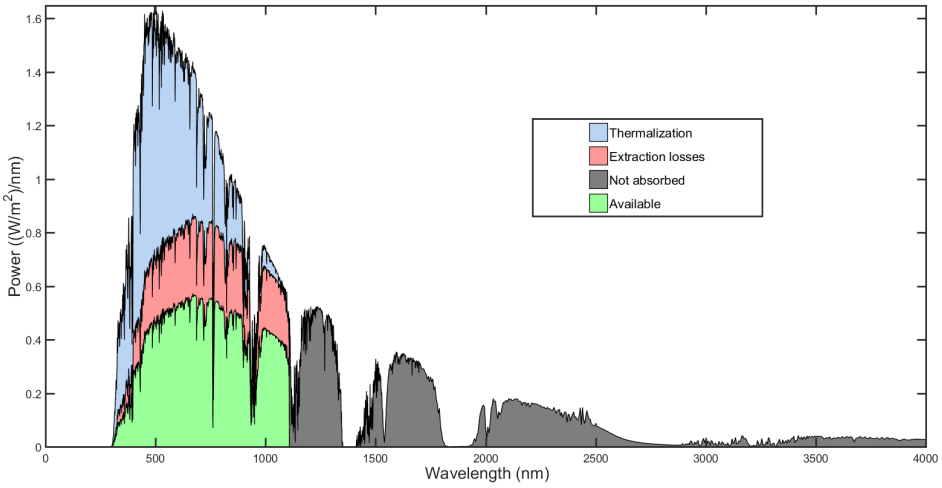

Figure 1.2: Visual representation of the origin of the losses of a silicon solar cell (1.1 eV band gap). The grey shaded area represents the losses caused by the inability to create charge carriers from photons with less energy than the band gap energy. The excess energy lost by thermalisation of electrons is depicted by the blue shaded area. The red area represents extraction losses occurring by radiative recombination and entropic losses.[8]

1.2 Spectral losses in PV

As can be seen from the visual representation of the losses considered by Shockley and Queisser shown in figure 1.2, three big losses can be distinguished in the solar spectrum. The first loss originates from the fact that incoming photons need an energy larger than the internal band gap of the semiconductor. All incoming photons with less energy (and therefore with a wavelength above a certain threshold) are not able to excite an electron into the conduction band and are therefore not absorbed. As a result, these photons are lost, constituting a loss of 19% of all energy provided by the sun.[8] This fraction is indicated by the grey shaded area in figure 1.2. The second loss that originates from the spectral shape is caused by photons with energy greater than the band gap. These photons create so-called hot carriers, which lose their energy relatively quickly by thermalisation. This is a process where an excited electron interacts with its surroundings, causing the electron to relax to the conduction band edge by dissipating its excess energy as heat. Due to the fact that a single photon can only excite a single electron (the quantum defect), all energy carried by photons that is greater than the internal band gap, is lost. This loss is indicated in figure 1.2 by the blue shaded area, composing a 33% loss.[8] Next to the spectral losses, extraction losses due to radiative recombination and entropic losses comprise a loss of 15%.

1.3 Beyond the Shockley-Queisser limit

Many approaches to exceed the Shockley-Queisser limit have been proposed throughout the years, with a variety of principles as their basis in circumventing the limit.[9–12] An important concept in overcoming the Shockley-Queisser limit, is that of the tandem solar cell,[13] already introduced in 1976. In the tandem solar cell structure, two or more semiconductor materials with different band gap energies (with $E_{bg,1} > E_{bg,2}$) are combined. By absorbing the high-energy photons in the first material and low-energy photons in the second, thermalisation losses can be reduced. This reduction arises because the excess energy of high-energy photons is lower, since they are absorbed more closely to the band gap. Therefore, by optimally adjusting the band gap energies of the semiconductor materials, the solar spectrum (figure 1.2) can be more efficiently absorbed. For the optimal combination of semiconductor materials in the two-cell tandem under AM1.5G illumination, efficiencies can improve to 42%.[14]

A tandem solar cell structure that has attracted a lot of attention recently, is the perovskite-silicon tandem solar cell, consisting of a perovskite top cell and silicon base cell. Research cell efficiencies of such architectures have already been shown to reach 28%[15] power conversion efficiency and could potentially exceed 30%.[16] Next to the increase in efficiency, the perovskite top cell can also be produced very cheaply, therefore being a valuable addition to the silicon base cell. However, since tandem solar cells require either current or voltage matching, tandem solar cells are strongly affected by spectral and temperature changes,[17] lowering the performance under realistic outdoor conditions. Furthermore, the long-term stability of perovskites is an issue that needs to be adressed, before perovskite-silicon tandem solar cells can become commercially viable.[18,19]

Another strategy to increase efficiency and ultimately overcome the Shockley-Queisser limit is spectral management. In spectral management, it is aimed to reshape the solar spectrum in such a way, that light can be absorbed more efficiently in a single-junction solar cell, rather than by suiting the solar cell optimally to the solar spectrum, as is the case for tandem solar cells. The purpose of spectral management is to reduce the spectral losses, either by photon upconversion, where two low-energy photons create one high-energy photon, or by photon downconversion, which refers to the reverse process. Consequently, with efficient up- or downconversion, the spectrum can be effectively tuned, resulting in a high intensity of photons with energy just above the band gap, minimalizing spectral losses. A big advantage of spectral management is that it requires no voltage or current matching, since a single-junction solar cell can be used. Therefore, spectral changes will have a less destructive effect than in the case of the tandem solar cell and is consequently a promising strategy to surpass the Shockley-Queisser limit.

1.3.1 Singlet Fission as downconversion process

An example of such a downconversing process is singlet fission.[20] Singlet fission materials are organic semiconductors that create two low-energy excitons from one high-energy exciton, generated by one high-energy photon. The concept of excitons in organic semiconductors is first introduced. Excitons are electrically neutral quasiparticles and consist of a bound state of an electron and hole, which are attracted to each other by the electrostatic Coulomb force. Excitons can form when a photon is absorbed by an organic semiconductor, exciting an electron from the HOMO (Highest Occupied Molecular Orbital) to the LUMO (Lowest Unoccupied Molecular Orbital). The electron and hole that make the exciton are both fermions, causing the exciton to have either antiparallel (singlet) or parallel (triplet) spin states. These exciton states in organic semiconductors are shown in figure 1.3. Excitons can be dissociated in electron-hole pairs, creating the charge carriers that form an electric current.[21–23]

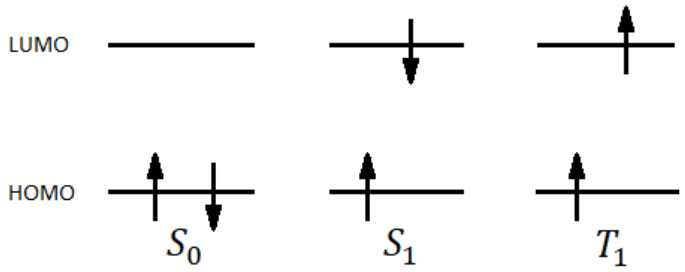

Figure 1.3: Schematic representation of existing exciton states in organic semiconductors. The electrons are located in the HOMO (Highest Occupied Molecular Orbital), but upon photoexcitation the electron can be excited into the LUMO (Lowest Unoccupied Molecular Orbital), leaving a hole behind. In the singlet ground state (S_0) and first excited singlet state (S_1) the electron and hole have antiparallel spin. In the excited triplet state (T_1), they have parallel spin.

The different spin states play a crucial role in a special kind of organic semiconductors, the singlet fission materials. The working principle of singlet fission is depicted in figure 1.4. Upon photoexcitation, an exciton in the singlet ground state (S_0) can be excited to the first excited singlet state (S_1), maintaining its spin quantum number of 0. Thereafter, it can form a correlated triplet pair ($^1(TT)$). Finally, this correlated triplet can converse to the final state of two independent triplet excitons ($T_1 + T_1$), both with spin quantum number of 1 and roughly half the excited singlet state energy. Generally, this reaction is written as[20]

$$S_0 + S_1 \Longleftrightarrow {}^1(TT) \Longleftrightarrow T_1 + T_1. \tag{1.1}$$

Since this singlet fission reaction can be much faster than the recombination rate of the excited singlet state (photoluminescence), singlet fission can be very efficient as a downconversion process, with triplet yields well over 100%.[23–25] Therefore, singlet fission provides a very promising way in order to circumvent the Shockley-Queisser limit, since high energy photons can in principle produce two triplet excitons, therefore reducing the quantum defect.[23,26–28] However, harvesting the triplet exciton energy is not as straightforward as it seems, since separation of the exciton into an electron and hole cannot happen inside known singlet fission materials itself.[29] Consequently, architectures need to be carefully designed to extract charge carriers efficiently in photovoltaic devices. We will discuss some photovoltaic devices using singlet fission materials below.

The first device based on a singlet fission material was reported in 2004 by Yoo et al.[30] Solar cells based on a pentacene/C_{60} heterojunction were reported with a power conversion efficiency of $2.7 \pm 0.4\%$ and an external quantum efficiency of 58±4%. This high quantum efficiency was ascribed to efficient exciton dissociation at the pentacene/C_{60} interface, as well as the reported large exciton diffusion length in pentacene. In 2009, high efficiency photodetectors based on the same pentacene/C_{60} heterojunctions were reported.[31] It was found that the quantum efficiency was increased by the singlet fission process by $45 \pm 7\%$, indicating that the previously reported[30] high quantum efficiency was presumably influenced by singlet fission.

Several other examples of photovoltaic devices with singlet fission-generated triplets contributing to the photocurrent have been reported. In 2012, Ehrler et al. reported singlet fission-sensitized infrared quantum dot solar cells, where a pentacene absorption layer as singlet fission material was combined with infrared quantum dot solar cells.[32] Internal quantum efficiencies exceeding 50% were reported, as well as power conversion efficiencies up to almost 1%. Furthermore, the authors showed that triplet excitons can be dissociated at the interface between the organic and inorganic materials.

In 2013, the first singlet fission solar cell exceeding 100% external quantum efficiency was reported, something that would never be possible with a conventional single-junction solar cell, showing the potential of singlet fission material as photovoltaic material. Congreve et al.[23] demonstrated a pentacene-based solar cell, with external quantum efficiency of 109% at the absorption peak of pentacene, corresponding to an internal quantum efficiency of 160% and triplet yield approaching 200%. A similar architecture was built in 2014 by Wu et al.,[33] where tetracene was used as absorber material. This device showed internal quantum efficiency of 127%, corresponding to a triplet yield of 153%. However, the authors argue that solar cells based on a singlet-fission material cannot be used to overcome the Shockley-Queisser limit, since the singlet fission process potentially doubles the photocurrent, but causes a halving of the open circuit voltage. Therefore, it is pointed out that it is highly desirable

to design a device that combines a singlet fission material with a conventional semiconductor material, preventing the loss of half the open circuit voltage.

The first device to combine singlet fission material and the conventional crystalline silicon solar cell was reported in 2017 by Pazos-Outón et al.[34] The authors demonstrate a pentacene-silicon parallel tandem solar cell with efficient photocurrent addition leading to an external quantum efficiency of 106% at the absorption peak of pentacene. However, since the pentacene and silicon solar cell are electrically connected in parallel, voltage matching is required, which restrains power conversion efficiency. Since the voltage of a pentacene ($E_{T_1} = 0.85$ eV) and silicon solar cell ($E_{bg} = 1.12$ eV) is not well-matched, power conversion efficiency could benefit from using a singlet fission material with higher triplet exciton energy, such as tetracene ($E_{T_1} = 1.25$ eV).

One way to avoid the efficiency losses in a singlet fission-silicon tandem solar cell associated with current or voltage matching, is to design a device with an architecture as depicted in figure 1.4. In this design, a singlet fission add-on layer is placed directly onto a conventional back-contacted silicon base solar cell, connecting the cells optically in series. The advantage of using a conventional silicon base cell is that silicon solar cell technology is well-known and already comprises 95% of the solar cell market.[35] Therefore, improving the efficiency of silicon solar cells by the addition of one singlet fission material film on the surface is highly desirable. In this architecture, the singlet fission material would act as a downconversion layer. By absorbing high-energy photons and converting them into two triplet excitons per absorbed photon, the singlet fission material can help reduce the quantum defect. Low-energy photons are transmitted and absorbed in the silicon base cell, where they can be absorbed efficiently. Since this architecture is designed to inject energy from the singlet fission material to the silicon absorber, it does not require voltage or current matching, therefore making it unaffected by temperature and spectral changes. The main challenge for this device however is to transfer the triplet exciton energy efficiently into the silicon absorber, where the charges can be extracted. Some evidence for such triplet energy transfer into crystalline silicon solar cells has been found,[36,37] but more research is needed for the realization of efficient singlet fission enhanced solar cells.

1.3.2 Energy transfer from Singlet Fission

As described above, the main challenge in using singlet fission as downconversion process is the transfer of the triplet energy to a low bandgap semiconductor, such as silicon. Proposed mechanisms for the transfer of this triplet energy include the transfer of triplet energy to intermediate quantum dots,[38] charge transfer and direct energy transfer.[36] This thesis will mainly focus on direct energy transfer, where energy of an exciton is directly transferred into silicon via either Dexter transfer or Förster Resonance Energy transfer

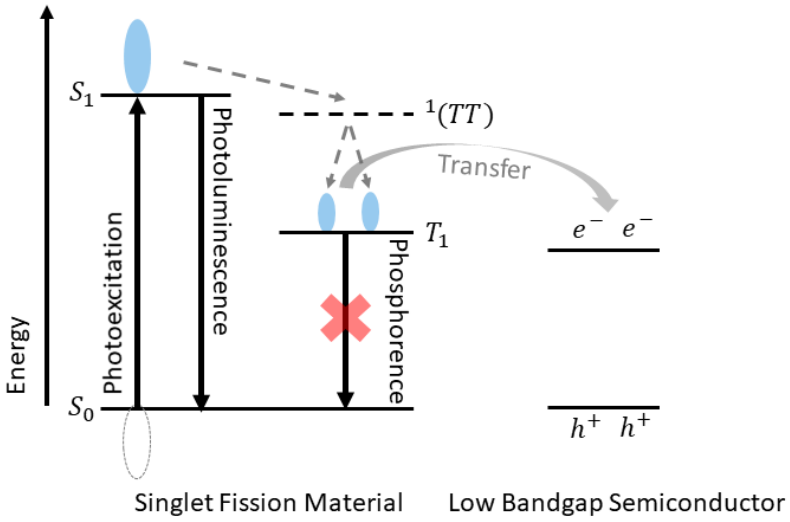

Figure 1.4: Jablonski-diagram of the singlet fission reaction process in an organic semiconductor combined with a low bandgap semiconductor. Upon photoexcitation, a singlet exciton is excited from the singlet ground state (S_0) into the first excited singlet state (S_1). This exciton can then directly recombine upon photoluminescence, but can also form a correlated triplet pair ($^1(TT)$), which can dissociate into two excitons in the excited triplet state ($T_1 + T_1$). Naturally, the inverse processes can also occur, annihilating two triplets to a singlet exciton, which can subsequently lose its energy by emitting a photon. Note that photoexcitation of an S_0 state to a T_1 state is spin-forbidden, as well as the reverse process of phosphorescence.

(FRET). Both transfer mechanisms are first introduced.

Dexter energy transfer

Dexter energy transfer was proposed in 1953 by Dexter[40] and is schematically shown in figure 1.5. It describes the non-radiative correlated transfer of an excited electron and hole from a donor molecule to an acceptor molecule. This exchange of charges means that an overlap of the wavefunction of donor and acceptor is necessary. Subsequently, the distances between donor and acceptor where Dexter energy transfer can take place are very small, typically smaller than 10 Ångstrom.[41] This can also be seen from the reaction rate constant for Dexter energy transfer, which is given by

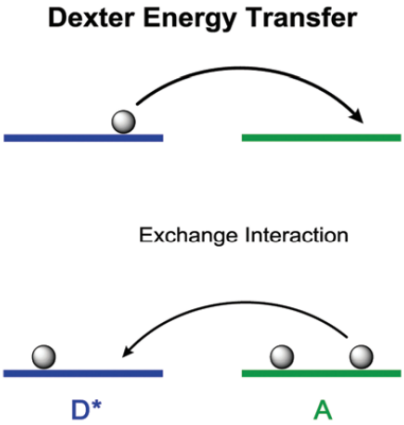

Figure 1.5: Schematic of Dexter transfer. Adapted from Strieth-Kalthoff et al.[39]

$$k_{dexter} \propto Je^{\frac{-2R_{DA}}{L}},$$

where R_{DA} is the distance between donor and acceptor molecule, J the spectral overlap integral and L is the sum of van der Waals radii. The exponential decay of the rate constant with distance shows that Dexter energy transfer is a short-range transfer process.

Förster Resonant Energy Transfer

Förster Resonant Energy Transfer (FRET) was described first by Förster in 1947[42] and is schematically shown in figure 1.6. As well as Dexter transfer, FRET is a non-radiative transfer process between an excited donor molecule and an acceptor molecule. However, FRET describes the energy transfer of an excited donor molecule to an acceptor molecule via Coulombic interaction, as opposed to Dexter transfer, where electrons and holes are transferred. The rate constant of FRET is given by[43]

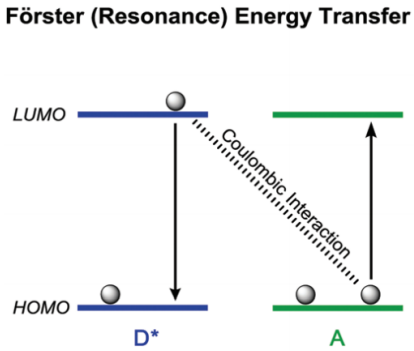

Figure 1.6: Schematic of FRET. Adapted from Strieth-Kalthoff et al.[39]

$$k_{FRET} = k_{D,0}\left(\frac{R_0}{R_{DA}}\right)^6,$$

where $k_{D,0}$ is the rate constant related to the lifetime in absence of an acceptor molecule, R_0 is the Förster Radius and R_{DA} the distance between donor and acceptor molecule. As can be seen from the formula for the FRET rate constant, this process is distance-limited, since the rate constant decays with the 6^{th} power. Generally, FRET can only effectively take place when the distance between donor and acceptor is less than 10 nm.[44] Furthermore, FRET is only possible as energy transfer mechanism for transfer processes that can also occur radiatively, that is via photon transfer. Therefore, only singlet energy transfer via FRET can occur.

1.3.3 Energy transfer in singlet fission silicon solar cells

Our intended architecture to investigate whether direct energy transfer takes place in a singlet fission enhanced silicon solar cell consists of a tetracene add-on layer as singlet fission material on top of a back-contacted silicon solar cell, with a direct interface between tetracene and silicon. The energy of a triplet exciton in tetracene is 1.25 eV, which means that energy transfer from the triplet exciton to silicon ($E_{bg} = 1.12$ eV) can take place. The proposed architecture is schematically shown in figure 1.7. An advantage of an architecture with add-on layer is that it does not require voltage or current matching, since excitons are dissociated in electrons and holes inside the silicon and can therefore directly contribute to the extracted current. Furthermore, an architecture with add-on layer can use any base silicon solar cell, for which the manufacturing processes are very well-known. The efficiency potential of such an architecture has been shown to be very promising.[27]

To utilize this potential of singlet fission enhanced solar cells, more insight needs to be gained in energy transfer mechanisms and their efficiencies. In this thesis, we aim to experimentally demonstrate the transfer of triplet energy

from tetracene into silicon in the above-described architecture with tetracene add-on layer. Methods include magnetic field dependent measurements of photocurrent and quantum efficiency measurements.

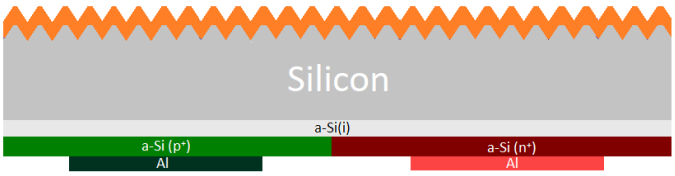

Figure 1.7: Intended architecture consisting of an interdigitated back-contact HIT solar cell with a tetracene add-on layer

2 | Theory

In singlet fission solar cells with architecture as in figure 1.7, charge that is eventually extracted can have very different origins. For instance, all light with energy larger than the silicon band gap energy, but smaller than the tetracene band gap, will be absorbed in the silicon and generate electron-hole pairs in that material. However, light with sufficient energy to excite an electron in the singlet fission material, will create singlet excitons, which can finally form two triplet excitons. Both these exciton types can transfer their energy to silicon via the earlier-described Dexter transfer (triplet excitons) or FRET (singlet excitons). In singlet fission solar cells it is important to determine what the origin of the eventually extracted charge carriers is, since only energy transfer from triplet excitons can contribute to reducing the quantum defect. To make the distinction between singlet and triplet exciton transfer in singlet fission solar cells, an experimental strategy based on Johnson-Merrifield theory[45] is commonly used. Johnson-Merrifield theory is introduced here.

2.1 Johnson-Merrifield theory

Johnson-Merrifield theory describes the behaviour of singlet fission-generated triplet excitons under the influence of a magnetic field.[45] Generally, triplet excitons are able to pass through the inverse reaction of the singlet fission process (equation 1.1), annihilating with another triplet exciton into an singlet exciton, which can subsequently fall back to the ground state, re-emitting a photon.[46] This process is called delayed fluorescence, in contrast to prompt fluorescence, which occurs when a singlet exciton directly falls back to the ground state without forming a triplet pair first. In 1967, it was discovered by Johnson and Merrifield that the process of triplet-triplet annihilation is influenced by the presence of a magnetic field.[47] More importantly, they showed a general dependence of the prompt and delayed fluorescence on the magnetic field strength, caused by the dependence of singlet and triplet exciton population on magnetic field.

This dependence on magnetic field of the singlet and triplet population is caused by the spin character of the $^1(TT)$ state in equation 1.1. In figure 2.1, a more detailed singlet fission reaction formula is shown.[23] The singlet fission process is shown to occur via an intermiate state of a spin-coupled correlated

triplet-pair ($(TT)^l$). Nine different spin-coupled triplet-pairs exist, indicated by $l = 1, ..., 9$, with different spin-singlet character, designated by the factor $|S_l|^2$. This singlet character $|S_l|^2$ of the correlated triplet-pair changes under magnetic field, in effect changing the rate constants at which the singlet fission reaction takes place, therefore shifting the balance in singlet and triplet exciton population. Note that for this particular singlet fission reaction in pentacene, triplet-triplet anniliation is not included, as delayed fluorescence has never been reported in pentacene.

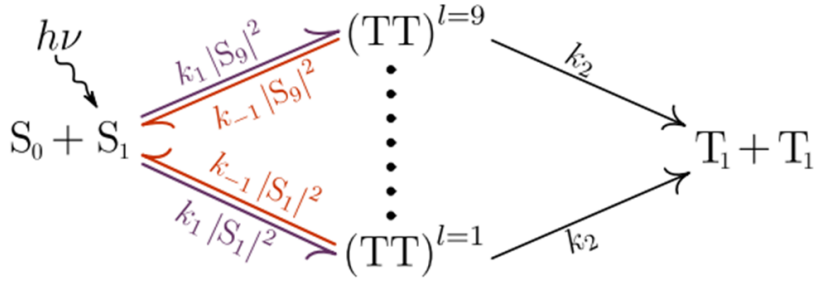

Figure 2.1: Singlet fission reaction scheme. Figure adapted from Congreve et al.[23]

The magnetic field effect is qualitatively shown in figure 2.2. Because singlet exciton population and triplet exciton population react differently to an external magnetic field, this effect can be used to analyze whether photocurrent in singlet-fission sensitized solar cells is originating from triplet or singlet excitons.[33]

Typical Johnson-Merrifield curves from experiments describe relative change in either photocurrent or photoluminescence as a function of magnetic field strength. In our case of a singlet fission solar cell, we measure the relative change in photocurrent, which can be written as

$$\delta_I(B) = \frac{I(B) - I(0)}{I(0)}, \tag{2.1}$$

where δ_I is the current modulation, $I(B)$ the current at a certain magnetic field B and $I(0)$ the zero-field current. In experiments, it is often the case that multiple light sources illuminate multiple absorber materials. In our device as shown in figure 1.7, the absorber layers comprise of the tetracene add-on layer for high-energy photons and silicon for low-energy photons. In such cases of multiple light sources and absorber materials, we can break formula 2.1 down into the individual current contributions originating from their absorber

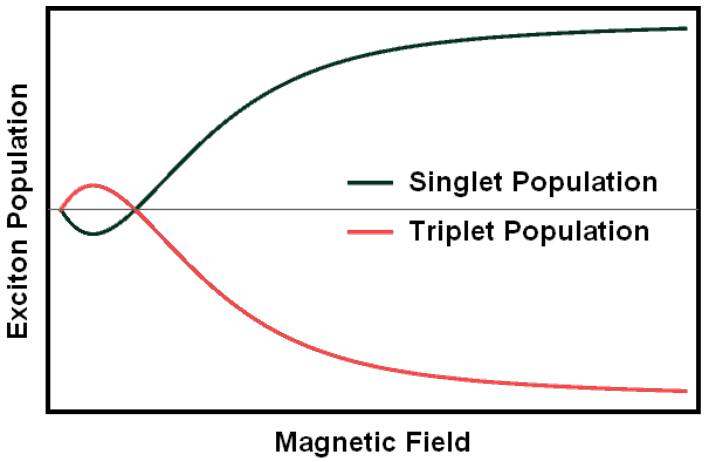

Figure 2.2: Qualitative plot of the magnetic field dependence of singlet and triplet population in a singlet fission material. Since photocurrent increases with increasing exciton population, this figure shows that photocurrent originating from triplet excitons slightly increases for small magnetic field, whereafter a significant decrease is visible for greater magnetic field. The opposite effect occurs for singlet induced photocurrent.

material and light source. For our silicon solar cell with a tetracene top layer (figure 1.7), illuminated by a white light source and a green laser, this becomes

$$\delta_I(B) = \frac{I^G_{Tc}(B) + I^G_{Si}(B) + I^W_{Tc}(B) + I^W_{Si}(B) - I^G_{Tc}(0) - I^G_{Si}(0) - I^W_{Tc}(0) - I^W_{Si}(0)}{I^G(0) + I^W(0)}. \tag{2.2}$$

In this formula, the absorber material is indicated by the subscript and the light source is given by the superscript. Since the current originating from the silicon absorber should have no magnetic field dependence, we assume $I_{Si}(B) = I_{Si}(0)$, which reduces equation 2.2 to

$$\delta_I(B) = \frac{I^G_{Tc}(B) + I^W_{Tc}(B) - I^G_{Tc}(0) - I^W_{Tc}(0)}{I^G(0) + I^W(0)}. \tag{2.3}$$

Since white light consists of light of all wavelengths, a part of the white light will be absorbed by the singlet fission material and will therefore have dependency on the magnetic field, such that $I^W_{Tc}(B) \neq I^W_{Tc}(0)$. However, in experiments, it is often useful that the magnetic field modulation of the photocurrent is only caused by one light source. To ensure this, we can filter all high-energy photons in the white light with a long-pass filter, such that no absorption takes place in the singlet fission material. This reduces equation 2.3 further to

$$\delta_I(B) = \frac{I^G_{Tc}(B) - I^G_{Tc}(0)}{I^G(0) + I^W(0)}. \tag{2.4}$$

2.2 External Quantum Efficiency

External quantum efficiency is a powerful tool to examine the performance of photovoltaic devices. Generally, it is defined as the ratio between the number of electrons extracted from a photovoltaic cell and the number of incident photons. We can write this as

$$EQE(\lambda) = \frac{J(\lambda)/q}{AMG1.5(\lambda) * \frac{\lambda}{hc}}, \tag{2.5}$$

where $J(\lambda)$ is the current density as function of the photon wavelength λ, q is the elementary charge and $AMG1.5(\lambda)$ is the solar power spectrum. From equation 2.5, we can immediately see that the external quantum efficiency of a conventional solar cell does not exceed 100%, since every photon is only able to excite one electron. However, in the case of successful downconversion of photon energy, external quantum efficiency can in fact exceed 100% for certain ranges of the spectrum and is therefore a powerful tool to analyze photovoltaic architectures aiming to surpass the Shockley-Queisser limit using photon downconversion.[23,33,34]

3 | Methods

3.1 Methods for device preparation

3.1.1 Removal of Silicon Nitride Anti-Reflection Coating

Heterostructure with intrinsic thin layer (HIT) interdigitated back contacted (IBC) silicon solar cells with random pyramid structure, provided by Energieonderzoek Centrum Nederland (ECN), were received coated by a silicon nitride anti-reflection coating (ARC). In order to make direct contact between the singlet fission material and the crystalline silicon, the silicon nitride anti-reflection coating was etched using a 40% hydrogenfluoride (HF) solution. Drops of HF were carefully placed on the silicon nitride front surface, making sure that no HF solution came in contact with the interdigitated back contacts. After roughly 10 minutes of etching, a sudden decrease in wettability of the surface occurred as the contact angle of the HF solution suddenly increased, because the top surface material composition has changed from silicon nitride to silicon. After this decrease in wettability occurred, the etching process was stopped by dipping the substrates in a series of two deionized water reservoirs and dry-blown with a nitrogen gun. After the etching process, the contact angle of water was determined at 70 ± 2 degrees (figure 3.1) using a home-built Schlieren set-up. This angle is typical for a randomly textured silicon surface, etched by a KOH solution.[48] This angle thus indicated that the front surface was now completely stripped of silicon nitride, exposing the randomly textured silicon surface.

3.1.2 X-ray photoelectron spectroscopy

To confirm the complete removal of silicon nitride at the front surface of the HIT-IBC cells, X-ray photoelectron spectroscopy (XPS) measurements were performed on cells before and after the etching process. Figure 3.2 shows both XPS spectra. A clear nitrogen peak is visible at 398 eV in figure 3.2a, which is generally attributed to the nitrogen atoms that are present in the silicon nitride layer.[49] After the etching process (figure 3.2b), this nitrogen peak has completely vanished, indicating that no nitrogen atoms are present in the top 10 nm of this device. From this, we conclude that we have successfully removed the silicon nitride layer and therefore exposed the randomly textured silicon

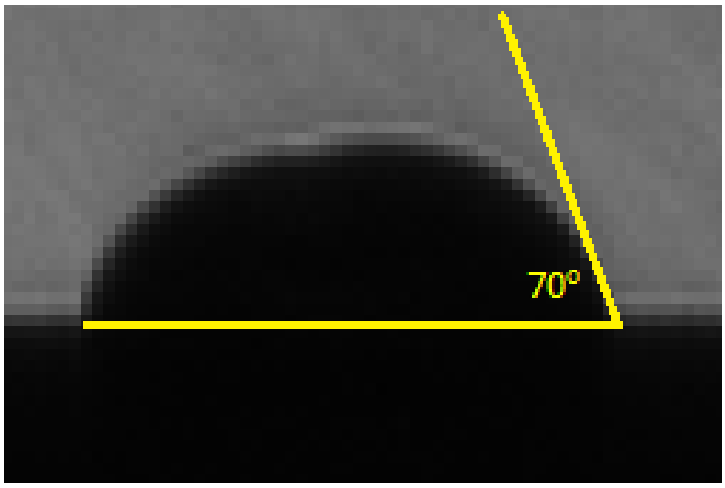

Figure 3.1: Image of a water drop on the front surface of an interdigitated back contacted solar cell, stripped of its silicon nitride anti-reflection coating. The image was captured using a home-built Schlieren set-up.

surface. Note that after the etching process, a fluoride peak has appeared at 684 eV. The importance of this will be discussed later.

3.1.3 Device fabrication with different interlayers

Devices with three different interlayers were prepared for tetracene evaporation. The first device was placed in a nitrogen-filled glovebox shortly after the HF removal of silicon nitride to prevent oxide from growing onto the silicon top surface. The second device was stored under ambient conditions for 7 days after the HF removal of silicon nitride to grow a thin native silicon oxide film. For the third device, the HF removal of silicon nitride was omitted. Therefore, this device has an 80 nm silicon nitride interlayer.

3.1.4 Thermal evaporation of Tetracene

The devices with above-described interlayers were affirmed to a sample holder suited for an Angstrom Engineering EvoVac thermal evaporator with double-sided carbon tape. Tetracene (Sigma-Aldrich, sublimed grade, 99.99% trace metals basis) was evaporated at an evaporation rate of 1 Å/s at a base pressure below $6 \cdot 10^{-7}$ Torr. Using a pythron stage, thickness gradients could be manufactured on single devices.

3.1.5 Device encapsulation

After tetracene evaporation, devices were attached to Thermo Scientific microscope slides (76x26 mm) with double-sided carbon tape in a nitrogen-filled glovebox. Along the edge of the device, silicone adhesive sealant (Loctite 5366) was applied to prevent oxygen from reaching the device surface. For a complete

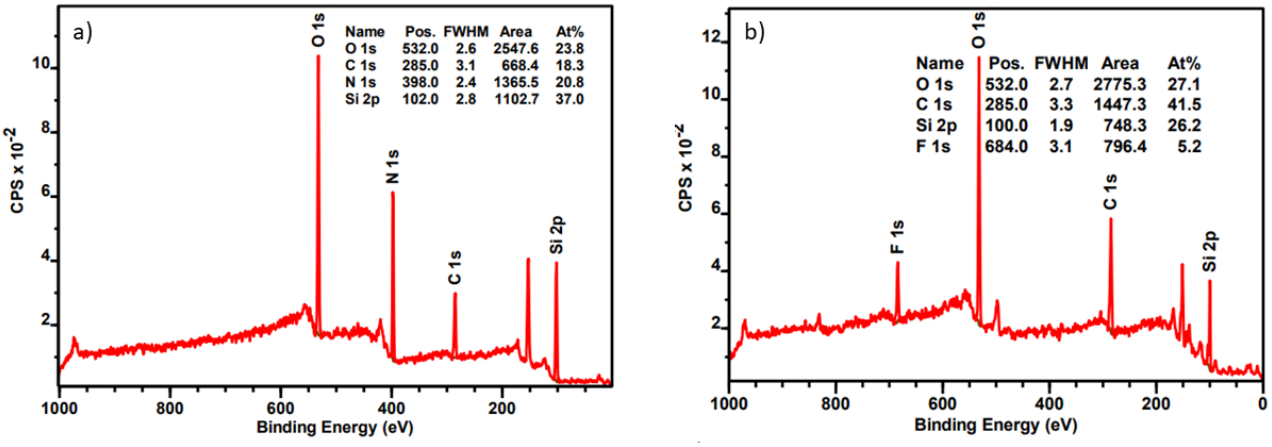

Figure 3.2: XPS measurements on HIT-IBC cells before (a) and after (b) removal of the silicon nitride top layer.

cure of the adhesive sealant, devices were stored for 24 hours under ambient conditions.

3.2 Methods for device performance characterization

3.2.1 Current-Voltage measurements

The current-voltage characteristics were determined by measuring photocurrent for different voltages using a Keithly 2636A Source Measuring Unit. For J(V)-curves under illumination, samples were illuminated by an Oriel 92250A solar simulator, calibrated with a silicon reference photodiode. For dark J(V)-curves, samples were covered with aluminium foil.

3.2.2 Magnetic field dependence of photocurrent in tetracene-silicon devices

To determine the magnetic field dependence of photocurrent, samples were placed in a GMW dipole electromagnet (Model 3470), generating a magnetic field up to 0.5T via the staircase method (figure 3.3). Photocurrent was measured for each step by a Keithly 2636A Source Measuring Unit and the photocurrent modulation was subsequently calculated according to equation 2.1. Samples were illuminated by a 520 nm diode laser to ensure efficient light absorption in the tetracene add-on layer. An absorption spectrum of a tetracene crystalline film is shown in figure 3.4, showing high absorption at 520 nm in a tetracene crystalline film. A white-light bias can be applied using a 100W halogen lamp.

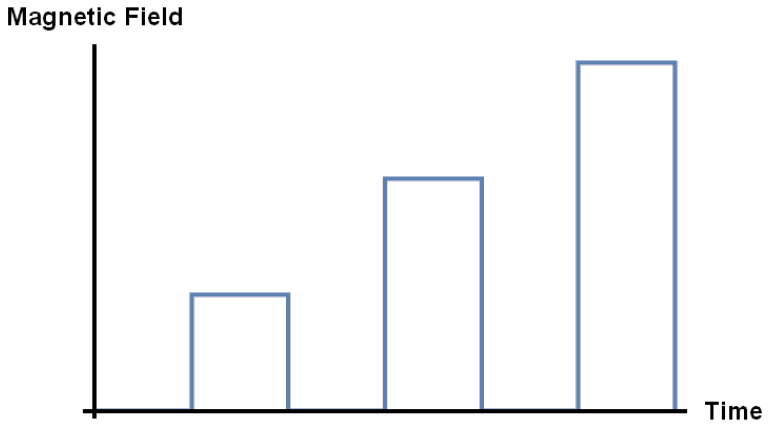

Figure 3.3: Magnetic field dependence of photocurrent determined by the staircase method. At each step of the staircase, photocurrent is measured. The magnetic field modulation of the photocurrent is subsequently calculated according to formula 2.1.

3.2.3 Quantum efficiency measurements

The external quantum efficiency is measured with a Newport Oriel QuantX-300 system, that provides external and internal quantum efficiency, as well as reflective losses in a 325 to 1800 nm wavelength range. The system (figure 3.5) consists of a Xenon lamp, which sends light through a chopper wheel onto a monochromator in order to select a certain wavelength. Light of this wavelength hits a beamsplitter, which sends light onto the sample as well as into the beam monitor. The signal of the sample is coupled into a lock-in amplifier together with the chopper frequency for an accurate measurement of the photocurrent. The reflection of the sample is collected by a reflectance monitor.

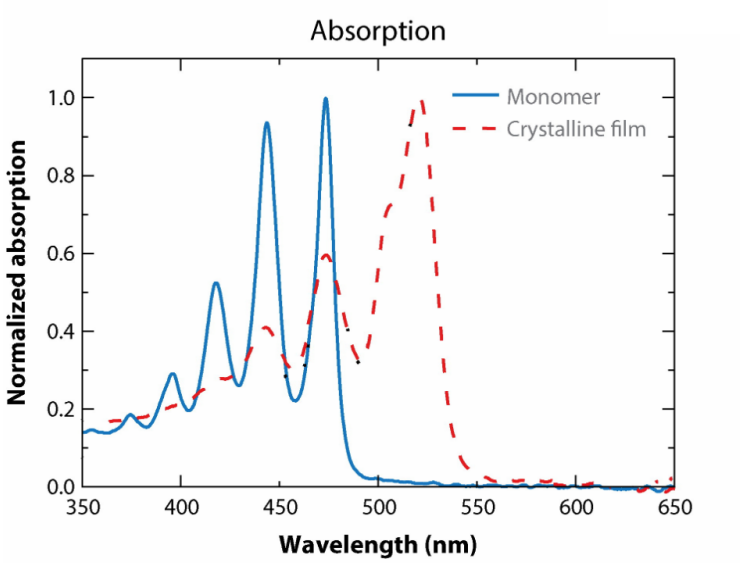

Figure 3.4: Normalized absorption spectrum of tetracene in solution (monomer) and crystalline film. Figure taken from Bardeen.[50]

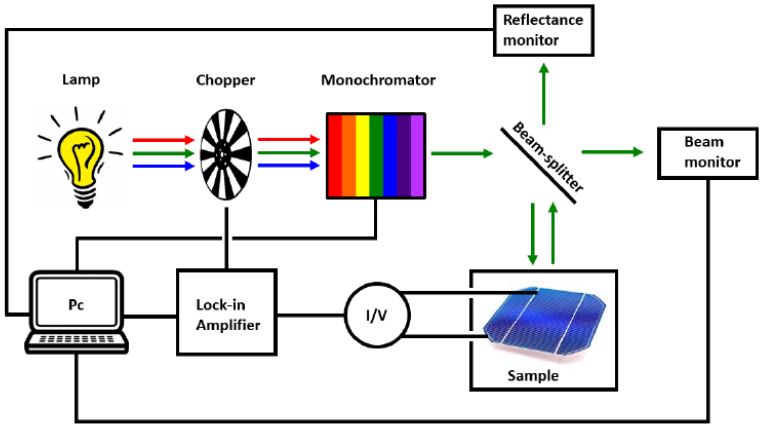

Figure 3.5: Schematic set-up of the Newport Oriel Quantum Efficiency QuantX-300 system. Figure adapted from van den Hoven.[51]

4 | Results and Discussion

4.1 J(V)-curves

To get insight into the performance of the devices throughout the manufacturing process, J(V)-characteristics were measured after each fabricating step. From the J(V)-characteristics, especially the short circuit current density (J_{sc}) is an important parameter here, since both the magnetic field-dependent photocurrent measurements and the quantum efficiency measurements require a sufficient current to yield reliable results. Figure 4.1 shows the characteristics of a single device throughout the manufacturing process. The device had an initial 14.1% power conversion efficiency as 15x45 mm HIT-IBC cell with a J_{sc} of 36.3 mA/cm^2. After removal of the silicon nitride anti-reflection coating and passivating layer, the short circuit current density significantly decreased to a J_{sc} of 9.7 mA/cm^2. The open circuit voltage also decreased as a result of increased surface recombination and decreased short circuit current, yielding a 3.8% power conversion efficiency. After evaporation of a 200 nm tetracene thin-film add-on layer, J_{sc} decreased further to a final 6.8 mA/cm^2. Although this is a sufficient short circuit current to perform the following device characterization experiments, the further decrease of the photocurrent as a result of 200 nm tetracene add-on layer already indicates that photocurrent does not increase as a result of triplets being generated in the singlet fission material, but rather decreases by parasitic absorption. This does, however, not exclude the possibility of triplet energy transfer from tetracene to silicon taking place, albeit with a low efficiency.

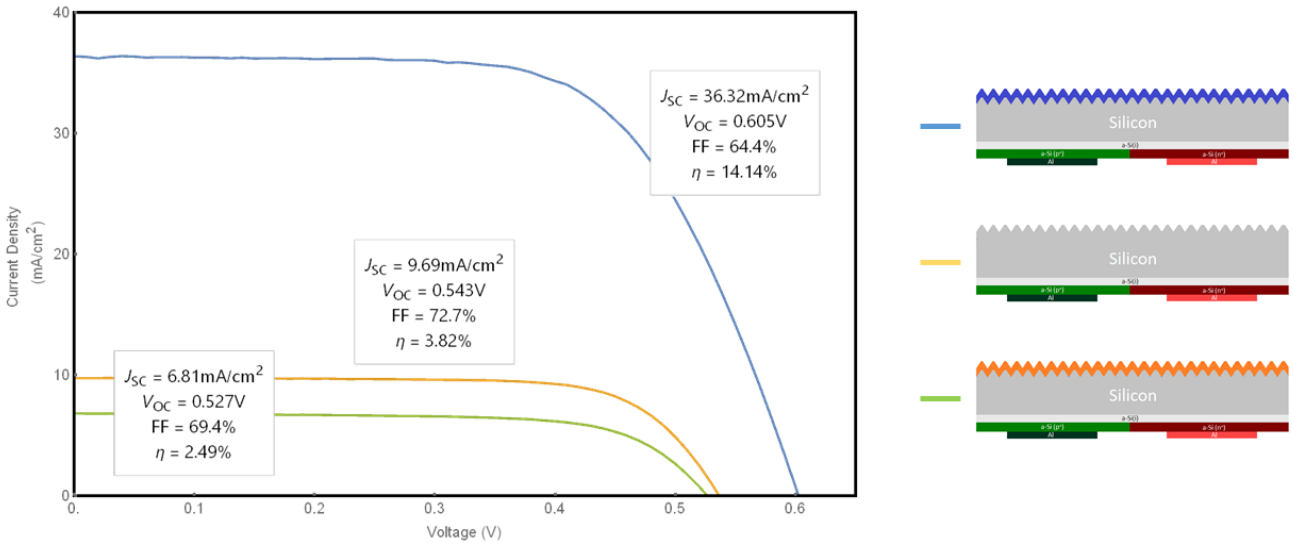

Figure 4.1: J(V)-characteristics of HIT-IBC cells throughout the device preparation process. The blue curve shows the J(V)-curve of a 15x45 mm HIT-IBC cell as received from ECN. The yellow curve shows the performance of the same cell without its silicon nitride anti-reflection coating and passivating layer. The green curve shows the J(V)-characteristic of our final device, with a 200 nm tetracene add-on layer on top of a silicon HIT-IBC cell.

4.2 Magnetic field-dependent photocurrent

Magnetic field-dependent measurements are an important tool in the field of singlet fission. Because magnetic fields shift the balance between the number of singlets converted to triplets in singlet fission materials, they can be used to distinguish whether photocurrent is originating from triplet or singlet excitons. We aim to use this technique to determine whether the photocurrent in our devices contains a contribution of current from the singlet fission material and to determine the spin character of this contribution. Three devices with interlayers described in section 3.1.3 that were initially prepared and measured are shown in figure 4.2.

4.2.1 Initial Johnson-Merrifield Curves

The magnetic field-dependent photocurrent of three architectures (figure 4.2) was measured shortly after device encapsulation. The results are shown in figure 4.3. A small initial decrease in photocurrent is clearly visible, whereafter the photocurrent increases and levels off at magnetic fields greater than 0.3 Tesla. This trend is therefore clearly corresponding to the change in singlet exciton population under magnetic field as depicted in figure 2.2, which means that the change in photocurrent is also originating from singlet excitons. These singlet curves can be explained either by direct singlet energy

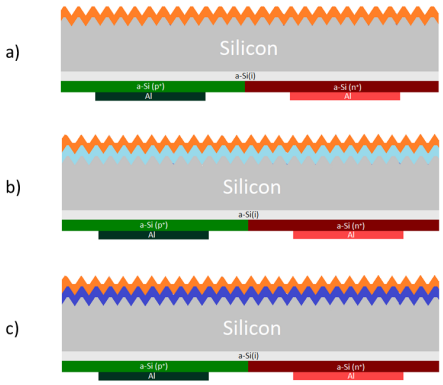

Figure 4.2: Three architectures have a base HIT-IBC silicon solar cell with a tetracene add-on layer. Device a) has a direct tetracene-silicon interface, whereas device b) has a native silicon oxide interlayer. For device c), tetracene was directly evaporated onto a base HIT-IBC cell, without removing the silicon nitride anti-reflection coating, and therefore has a 80 nm silicon nitride interlayer.

transfer or by the process of photon transfer. Since the devices with exciton blocking interlayers show an identical response to magnetic fields as the device with direct tetracene-silicon interface, we can exclude the possibility of direct exciton energy transfer via Dexter transfer or FRET. This is because these energy transfer mechanisms heavily depend on distance between donor and acceptor, which is too large in the devices with exciton blocking interlayers (2 nm for native silicon oxide and 80 nm for silicon nitride) for direct energy transfer to occur, since Dexter transfer typically takes places at distances smaller than 10 Å and FRET can only happen at distances smaller than 10 nm.[41,44] Therefore, we attribute the magnetic field response to photon transfer, an indirect energy transfer mechanism occurring from prompt fluorescence, a radiative recombination process where the singlet exciton in tetracene emits a photon which is subsequently absorbed in the silicon. Since the results appear to be identical for devices with and without blocking interlayers, we assume that photon transfer is also the mechanism of the singlet energy transfer in devices with direct tetracene-silicon interface.

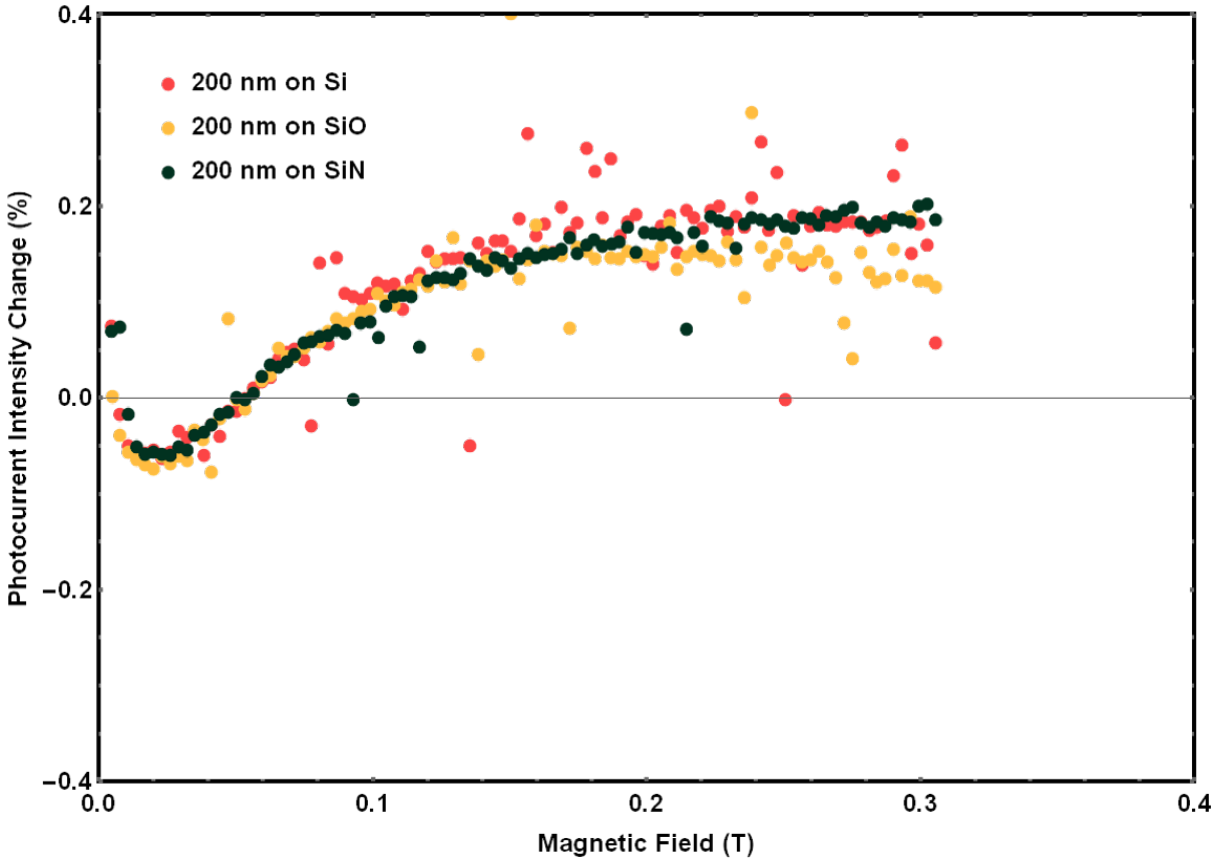

Figure 4.3: Magnetic field dependent measurements on photocurrent of devices schematically shown in figure 4.2. The red curve is measured on the device of figure 4.2a with a direct tetracene-silicon interface and shows a magnetic field effect corresponding to singlet energy transfer (figure 2.2). The yellow and dark green curves correspond to the devices with exciton-blocking interlayers shown in figure 4.2b and 4.2c respectively and both show behavior corresponding to singlet transfer.

The measurements shown in figure 4.3 all yielded clear magnetic-field response corresponding to singlet energy transfer. A judgement about the quality of a magnetic field-dependent photocurrent is based on several features typical for Johnson-Merrifield curves. First of all, the curve has to start at the origin, by definition of equation 2.1. Secondly, a small decrease/increase in singlet/triplet concentration at low magnetic fields ($0 < B < 0.05T$, see figure 2.2) occurs. The third feature is the zero crossing at $B \approx 0.05T$ and the last feature is the leveling of the curve at magnetic fields greater than $0.2T$. From figure 4.3, it can be seen that these four features are all present in the magnetic field-dependent photocurrent measurements corresponding to singlet energy transfer.

4.2.2 Aged Johnson-Merrifield Curves

After initial measurements of the magnetic field-dependent photocurrent as described above, devices were stored under ambient conditions and remeasured after a waiting time of 6 weeks. The results are shown in figure 4.4. For the devices with blocking interlayers, the results are identical to the initial measurement, shown in figure 4.3. However, the device with direct tetracene-silicon interface shows an inversed curve, with a small initial increase in photocurrent at small magnetic fields and a decrease in photocurrent at high magnetic field. This curve is corresponding to triplet exciton population as depicted in figure 2.2, which means that the change in photocurrent is originating from triplet excitons. The four above-described features by which we assess the Johnson-Merrifield curves are clearly present in figure 4.4, thus giving a good indication that triplet energy transfer takes place.

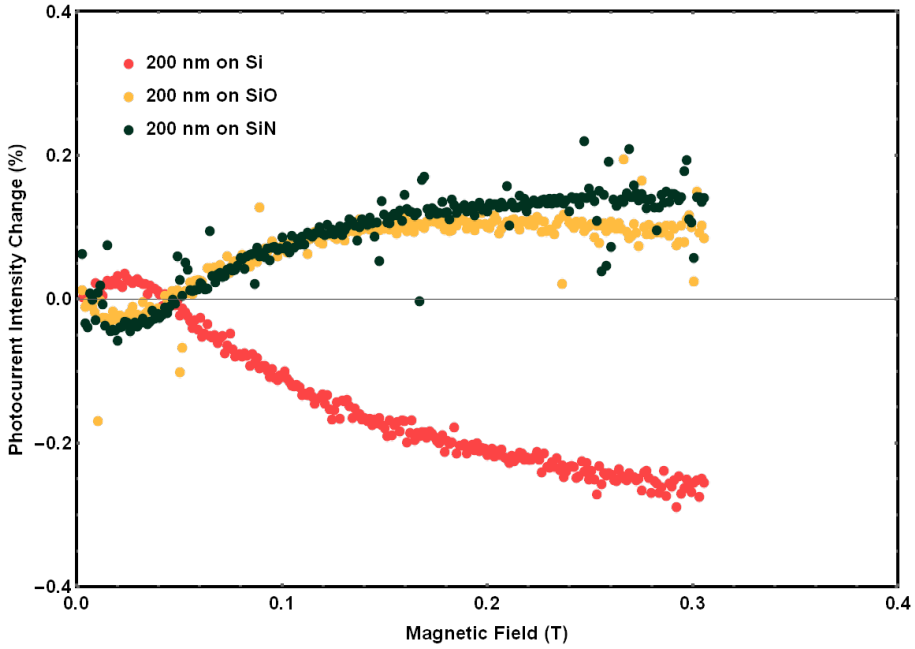

Figure 4.4: Measurements on magnetic field-dependent photocurrent of devices schematically shown in figure 4.2 after an aging time of 6 weeks. As opposed to the result in figure 4.3, the behavior of the device shown in figure 4.2a is now inversed and shows a magnetic field response corresponding to triplet energy transfer. The yellow and dark green curves correspond to the devices with exciton-blocking interlayers shown in figure 4.2b and 4.2c respectively and have not changed magnetic field response, both still showing singlet transfer.

The triplet energy transfer, however, cannot be attributed to photon transfer as before. Photon transfer that would yield this triplet curve should namely be originating from phosphorescence, where the triplet exciton emits a photon, or from delayed fluorescence, where two triplets recombine to one singlet, which in turn radiatively recombines. These processes are, however, very inefficient

in tetracene. Moreover, with this explanation, the devices with exciton blocking interlayers should yield identical results, as was the case before with singlet photon transfer. Therefore, the magnetic field effect for the device with direct tetracene-silicon interface is a strong indication for direct energy transfer and therefore a contribution to the current from triplet excitons.

However, other explanations for the appearance of this curve need to be considered. A potential origin of this magnetic field effect is trap state filling at the interface by triplets. It might also be that triplets, instead of transferring their energy to silicon, dissociate at the tetracene-silicon interface such that one of the charge carriers travels into the silicon, while the other one stays in the tetracene. This would lead to an accumulation of charges at the silicon surface, in effect creating a front surface field (FSF) passivation. This effective front surface field passivation improves the solar cell and is caused by triplets and would therefore yield a Johnson-Merrifield curve of the same shape, as would the earlier mentioned trap state filling.

4.2.3 Johnson-Merrifield Curves with white-light bias

Trap state filling and FSF passivation effects can both be differentiated from triplet energy transfer by a light-soaking experiment, which is schematically depicted in figure 4.5. In addition to the green laser, the device is soaked by another light source with higher power and wavelengths longer than 550 nm to ensure that the light passes trough the tetracene top layer. Subsequently, the light excites charges in the silicon, enhancing the charge density at the silicon surface. This charge density will lower the relative contribution to the front surface field passivation from the triplets from tetracene, as the total charge density is increased. This would consequently have destructive effect on the magnetic field dependency of the photocurrent, when it is caused by the formation of a front surface field of dissociated triplets at the tetracene-silicon interface. The same destructive effect should happen when the magnetic field effect is caused by trap state filling at the surface, since the enhanced charge density in silicon should also fill the trap states, lowering the relative contribution from triplets. However, when the triplets would transfer their energy into the silicon, only a decrease in current modulation by the addition of current from a different light source would be expected, according to equation 2.4.

A white-light bias was applied using a focused 100W halogen lamp with a 550 longpass filter to ensure aborption in silicon. The magnetic field-dependent photocurrent was measured twice, once with illumination from just the laser and once with illumination from both light sources. The results are shown in figure 4.6. This figure shows that the magnetic field effect decreases for illumination with both light sources (yellow curve) in comparison to the magnetic field effect for illumination with only the laser diode (red curve). If this decrease in current modulation only originates from the addition of an extra light

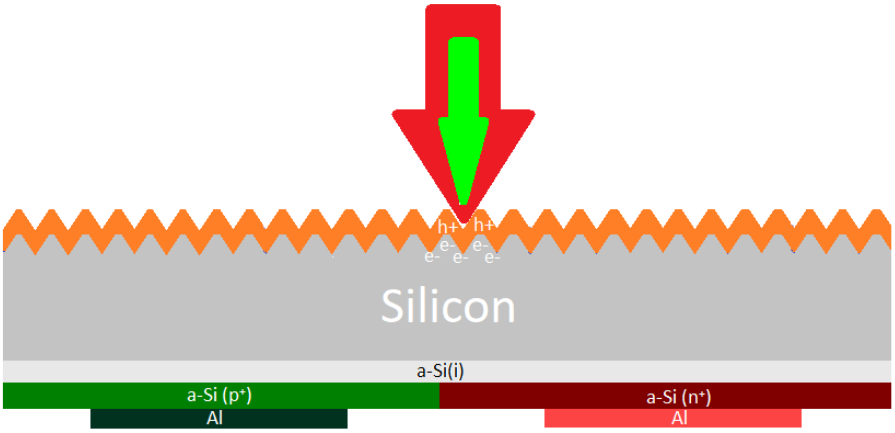

Figure 4.5: Schematic view of the above proposed lightsoaking experiment, where the device is illuminated by a 520 nm diode laser and a 550 nm longpass-filtered white light at the same time. This filtered white light only excites charges in the silicon, increasing charge density at the interface, reducing the triplet charging effect that was described above.

source and FSF passivation effects or trape state filling play no role, equation 2.4 should suffice in describing the magnetic field effect from both light sources (yellow curve in figure 4.6). Therefore, we measured the steady-state current generated by the only halogen lamp at zero-field and took this current as $I^W(0)$ in equation 2.4. Secondly, we took the data from the measurement that was illuminated by the laser only as $I_T^G c(B)$, $I_T^G c(B)$ and $I^G(0)$ to calculate the magnetic field modulation according to equation 2.4. As shown in figure 4.6, combining these two measurements mathematically yields the same curve as the measurement where the device was illuminated by both the laser and halogen lamp. This observation indicates that the front surface field passivation effect or trap state filling at the surface play no role and that triplet energy transfer from tetracene to silicon is taking place.

4.2.4 Oxygen as cause of triplet energy transfer

We have now established that triplet energy transfer can take place in a device with direct tetracene-silicon interface after an aging time of 6 weeks. An important question is the question of what process happens during this aging time, that could take such a long time. An important factor in answering this question, can be found in a comparison between the magnetic field-dependent photocurrent of an encapsulated device that has been aged under a nitrogen atmosphere and an encapsulated device that has been stored under ambient conditions, both with direct tetracene-silicon interface. For the device that was stored in ambient conditions, the inversion of the magnetic field effect

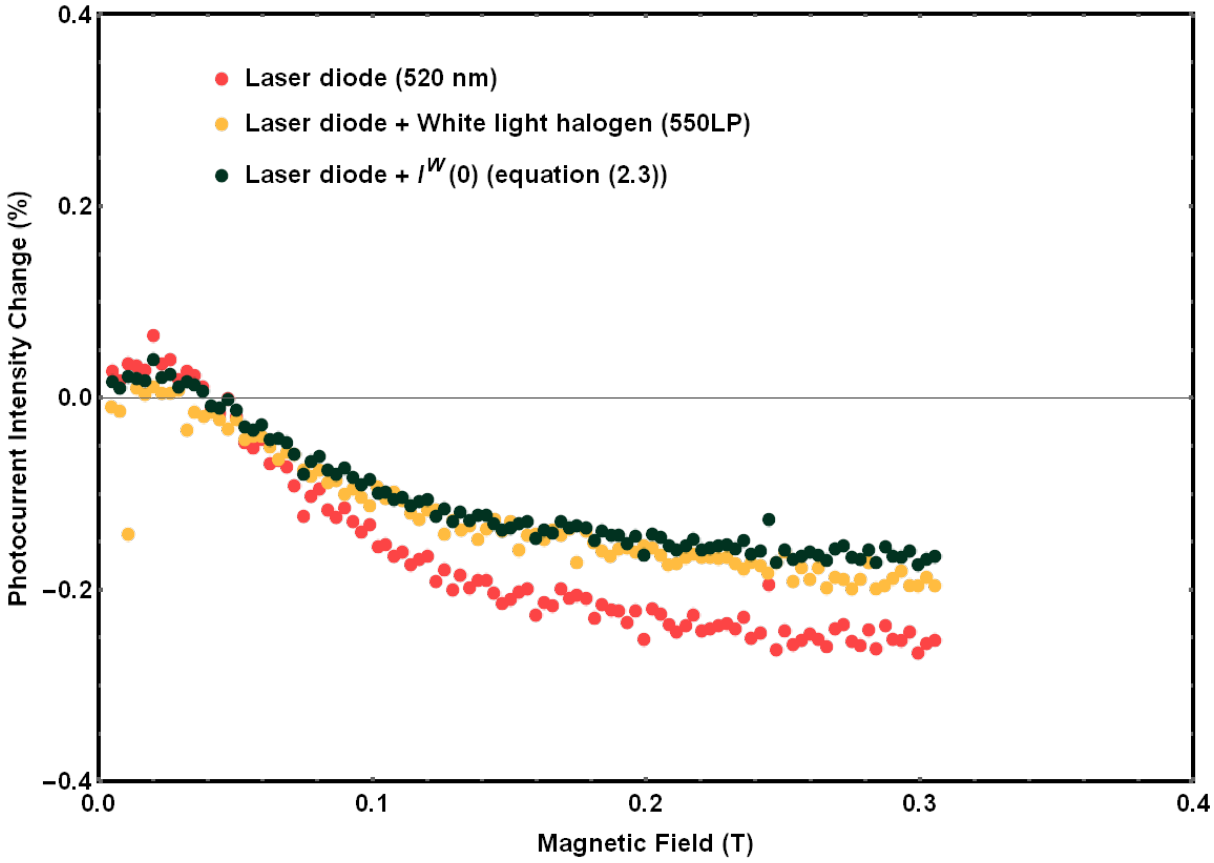

Figure 4.6: Measurements on magnetic field-dependent photocurrent originating from laser diode illumination (red curve) and combined illumination from a laser diode and filtered white light halogen lamp (yellow curve). The dark green curve shows the data from the illumination with laser diode exclusively, combined with the steady current arising from illumination with the white light halogen lamp according to equation 2.4.

occurred, as shown in figure 4.3 and 4.4. However, for the device stored in a nitrogen atmosphere, this inversion did not take place. This raises the expectation that the oxygen present in ambient atmosphere is playing an important role in the process of inversion. This would also explain the long aging time, since the devices were encapsulated inside a nitrogen-filled glovebox with an adhesive sealant. It might be that the encapsulation has not been completely preventing oxygen from reaching the device surface, but rather slowed the exposure to oxygen, thereby prolonging the aging time to 6 weeks.

To confirm the hypothesis that oxygen is an important factor in the aging process, we propose to repeat the magnetic field-dependent photocurrent experiment. However, this time, the encapsulation step should be omitted. By continuously measuring the magnetic field effect, we hope to get more insight into the aging process. If the aging process is indeed induced by oxygen exposure, the aging time should be significantly lower during this experiment. Preliminary results shown in figure 4.7 confirm that this is indeed the case. We observe a magnetic field effect corresponding to singlet transfer initially, but after storage in ambient conditions without encapsulation for 5 days, the inversion was observed. These results are a strong indication that oxide growth plays an important role in the facilitation of triplet energy transfer from tetracene to silicon.

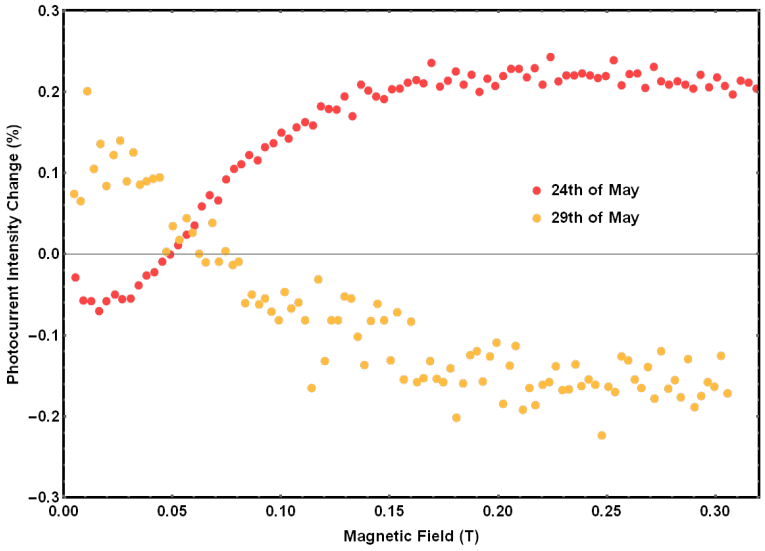

Figure 4.7: Magnetic field effect for a device measured after device preparation (red curve) and after an aging time of 5 days under ambient conditions (yellow curve).

4.3 External Quantum Efficiency measurements

4.3.1 Quantum efficiency of device with triplet energy transfer

Previous results indicate that in devices with direct tetracene-silicon interfaces, triplets from tetracene contribute to the extracted current from the silicon base solar cell after a certain aging time. More insight into the magnitude of this contribution can be gained from quantum efficiency measurements. Since tetracene can in principle produce two charge carriers for every absorbed photon, the quantum efficiency of our device with direct tetracene-silicon interface should exceed the quantum efficiency of the silicon base cell, in case of ideal transfer efficiency. To examine the influence of the thickness of the tetracene add-on layer, quantum efficiency measurements were performed on aged devices with different tetracene thickness. The results are shown in figure 4.8.

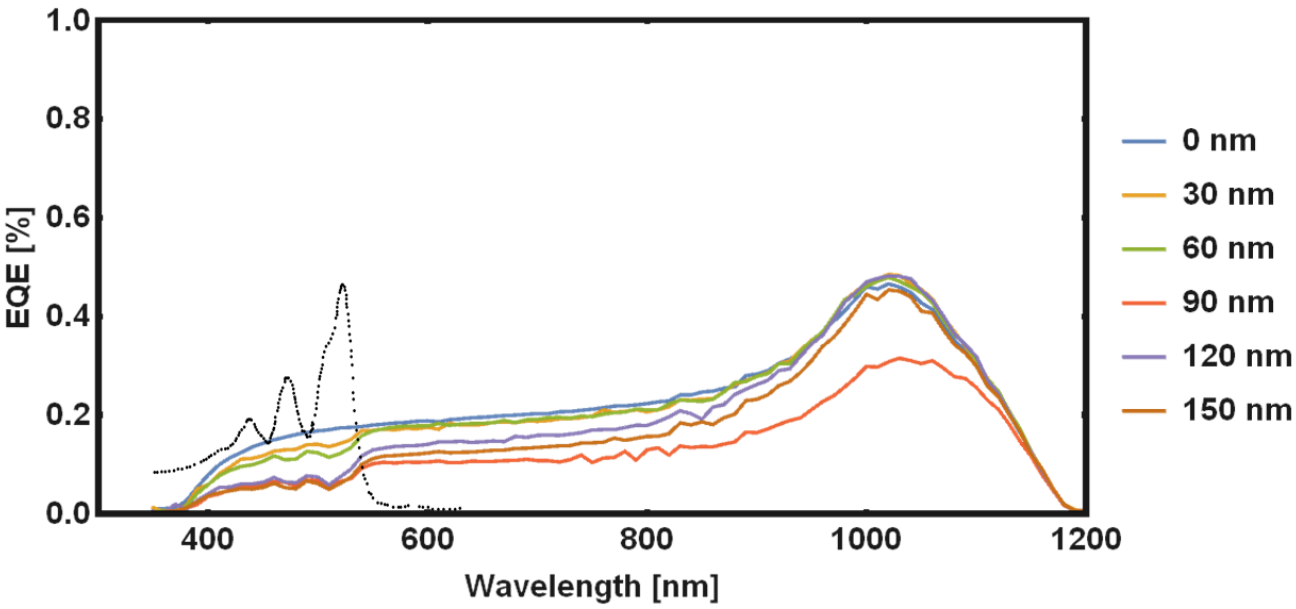

Figure 4.8: External quantum efficiency for an aged device with direct tetracene-silicon interface. Tetracene films of different thickness were evaporated on one device in a range of 0 to 150 nm. The black dashed line represents the normalized absorption spectrum of a crystalline tetracene film.

The results show a decrease in the absorption range of tetracene (dashed black line) with increasing thickness of the tetracene add-on layer. Therefore, we attribute this decrease in quantum efficiency to parasitic absorption in tetracene. This becomes even more clear when we look at a magnification of this wavelength range in figure 4.9, while adding an absorption spectrum of tetracene crystalline film in the figure to indicate correspondence between the absorption peaks of tetracene and the dips in quantum efficiency of the device.

A normalization to the measured value at 600 nm was carried out, since the quantum efficiency is hugely dependent on the location of the measurement. This normalization will be discussed in more detail in section 4.3.2.

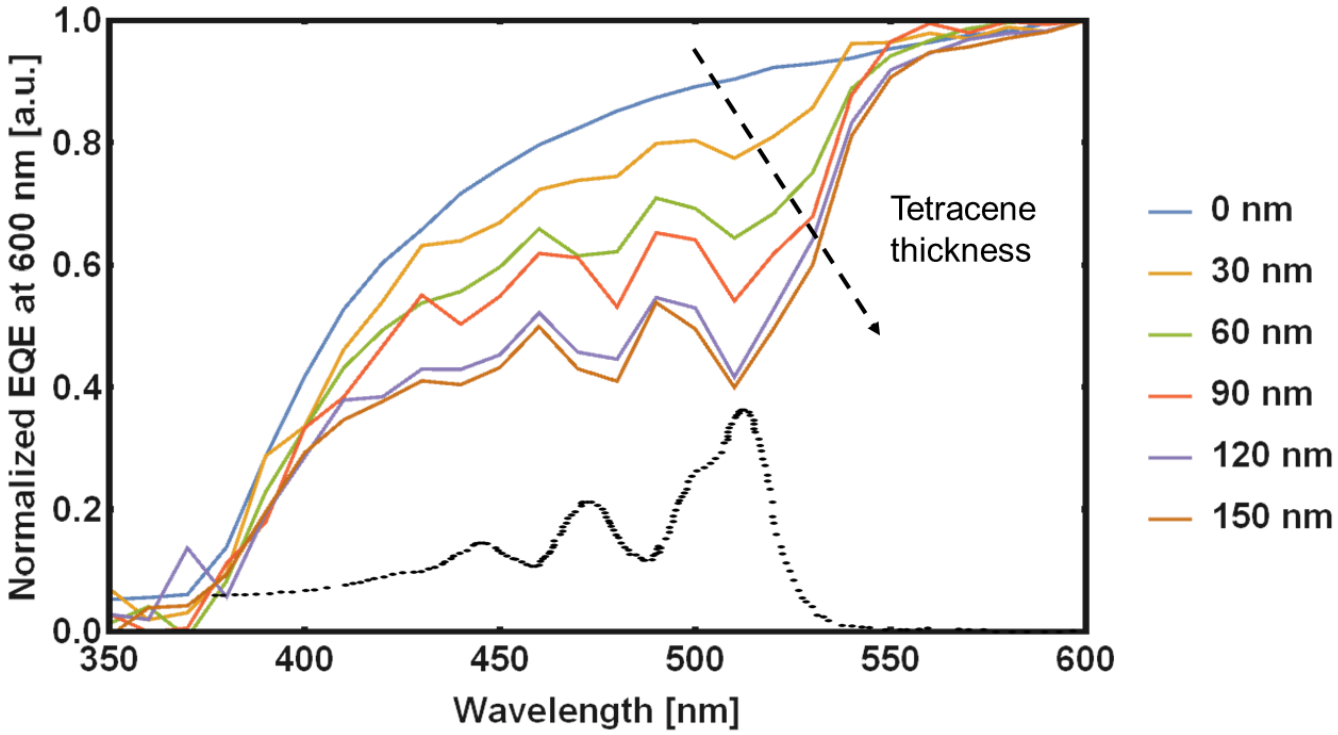

Figure 4.9: A zoom-in on the quantum efficiency of a device with direct tetracene-silicon interface in the absorbing wavelength range of tetracene, normalizing the quantum efficiency to their value measured at 600 nm. A clear negative correlation between tetracene film thickness and quantum efficiency is visible indicating parasitic absorption as the dominant effect. An absorption spectrum of a crystalline tetracene film is represented by the black dashed line.

From figure 4.8, we notice that the quantum efficiency spectrum does not have a shape corresponding to other tetracene-silicon solar cells reported in literature.[36] We attribute the shape to poor surface passivation quality after the HF etching step during device preparation. This assumption is backed up by the shape of the quantum efficiency spectrum of a device with no tetracene, the blue curve shown in figure 4.8. This shape shows an increasing quantum efficiency with increasing wavelength. Since light with shorter wavelength is generally absorbed closer to the surface than light with higher wavelength, shorter wavelengths would suffer more from bad surface passivation, as becomes clear from the quantum efficiency spectrum.

The results from quantum efficiency measurements shown in figure 4.8 show that parasitic absorption decreases photocurrent, confirming the indication

from the J(V)-measurement that the tetracene add-on layer does not increase the short circuit current by efficient downconversion. However, the results do not exclude the possibility of triplet energy transfer taking place. It might be that the conversion of triplet excitons to photocurrent is occurring with low efficiency and is therefore not visible as an increase in quantum efficiency. In order to quantify this exciton-photocurrent conversion yield, we need to look at the quantum efficiency of the device before and after the aging time, where it went from showing photon transfer to triplet energy transfer.

4.3.2 Comparison of devices before and after aging

To quantify the contribution of triplets to the photocurrent, measurements on quantum efficiency have been performed on samples before and after they were aged. The results are shown in figure 4.10. A significant increase in quantum efficiency is visible in the absorbing wavelength range of tetracene, however we cannot ascribe this to a contribution of triplet transfer. From figure 4.10, we can see that the quantum efficiency is also higher in the spectrum where tetracene does not absorb, and therefore cannot have an effect on the quantum efficiency. Consequently, we ascribe the apparent increase in quantum efficiency to the observation that quantum efficiency measurements are very dependent on measurement spot.

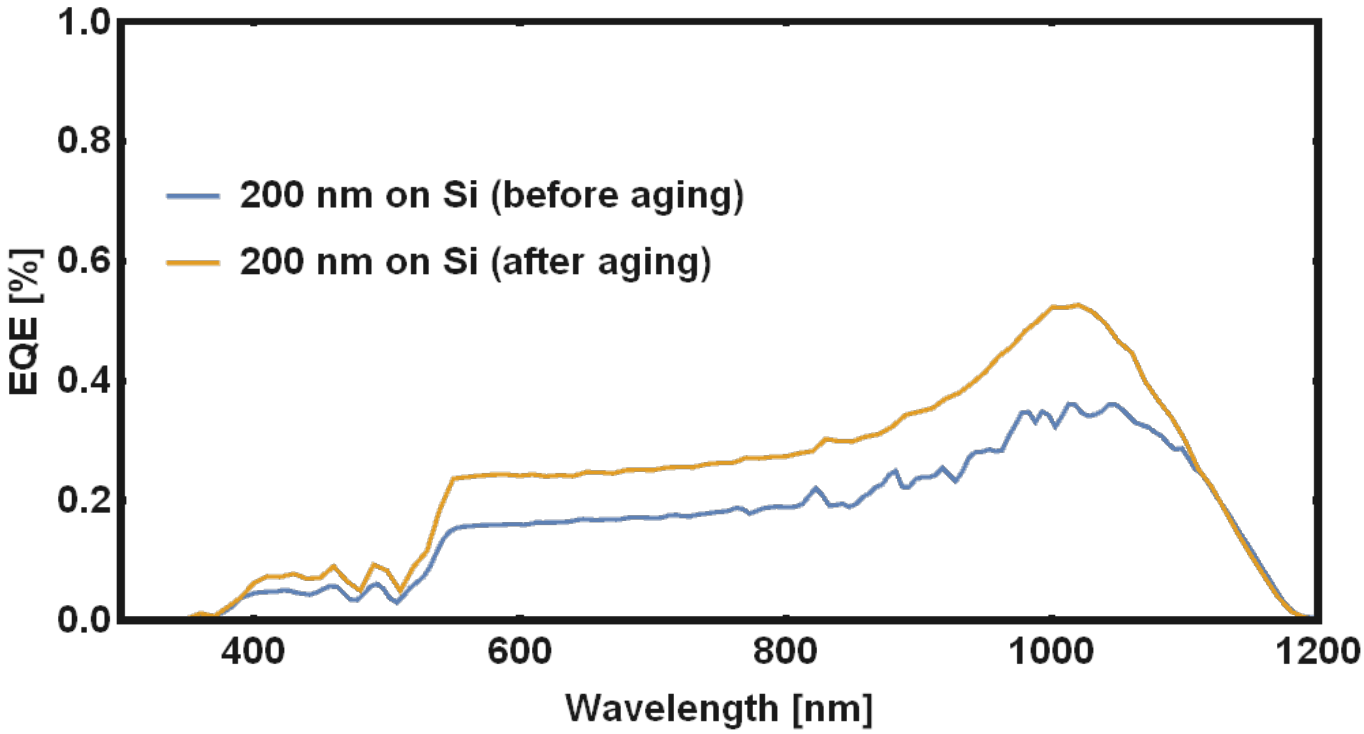

Figure 4.10: External quantum efficiency for a device with direct tetracene-silicon interface with a tetracene film thickness of 200 nm before and after an aging time of 6 weeks.

For a definitive conclusion about a possible increase in quantum efficiency in the absorbing range of tetracene, we look at a magnified figure of this exact range. To correct for the dependency on measurement location, we normalize both spectra to their values measured at 600 nm. The results are shown in figure 4.11. This figure shows that there is no significant increase in quantum efficiency in the absorbing range of tetracene. Consequently, we expect that the triplet yield contributing to photocurrent, following from figure 4.4, will be smaller than 5%.

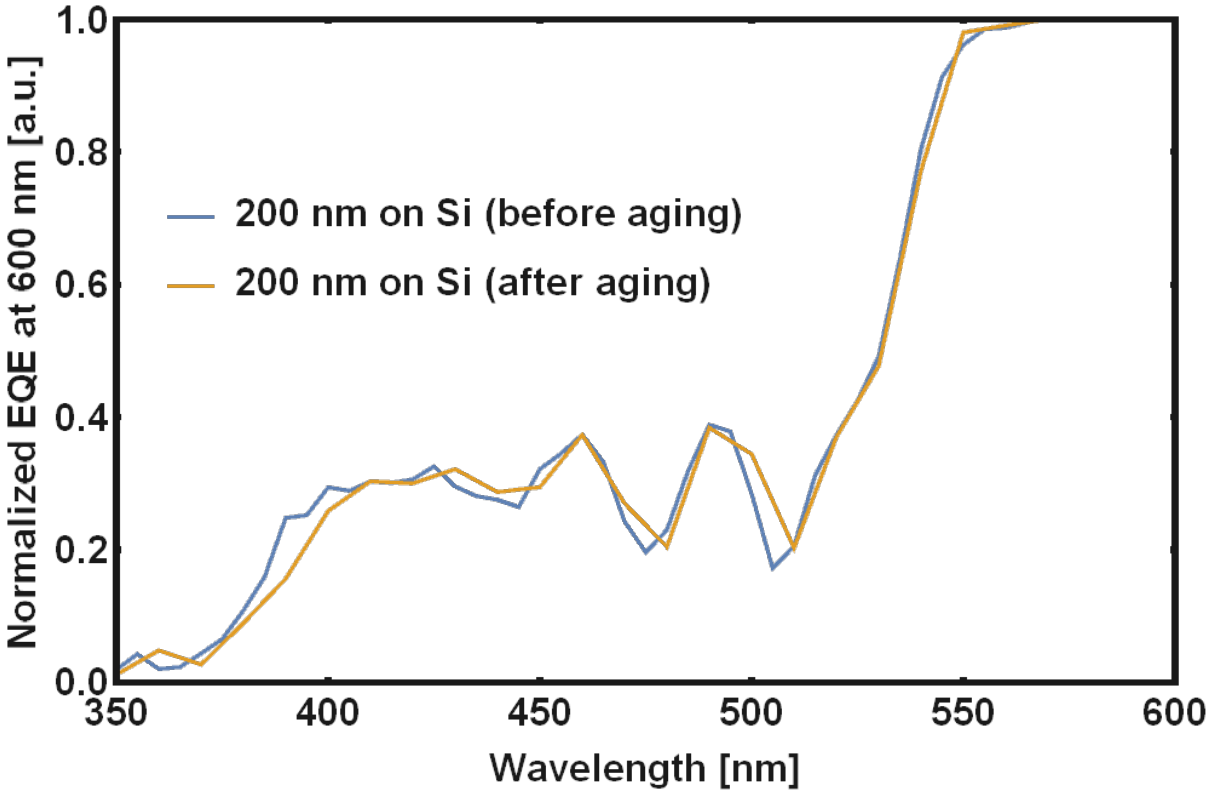

Figure 4.11: A zoom-in on the quantum efficiency before (blue curve) and after (yellow curve) the aging process of a device with direct tetracene-silicon interface in the absorbing wavelength range of tetracene. The quantum efficiency is normalized to their value measured at 600 nm to correct for the dependency of the quantum efficiency on spot location. No significant increase in quantum efficiency is visible after the aging process.

As mentioned before, to get conclusive results about the quantum efficiency measurements, a normalization was necessary. This follows from figure 4.12, where two measurements on quantum efficiency were done on the same device (HIT-IBC solar cell, as received from ECN, corresponding to the blue curve of figure 4.1), yet at different locations. Figure 4.12 shows clearly that the quantum efficiency is very dependent on measurement location. Location 2 was located slightly closer to the cut edge of the device, which is (as opposed to the top surface) not passivated and therefore more prone to surface recombination, having a very large effect on quantum efficiency.

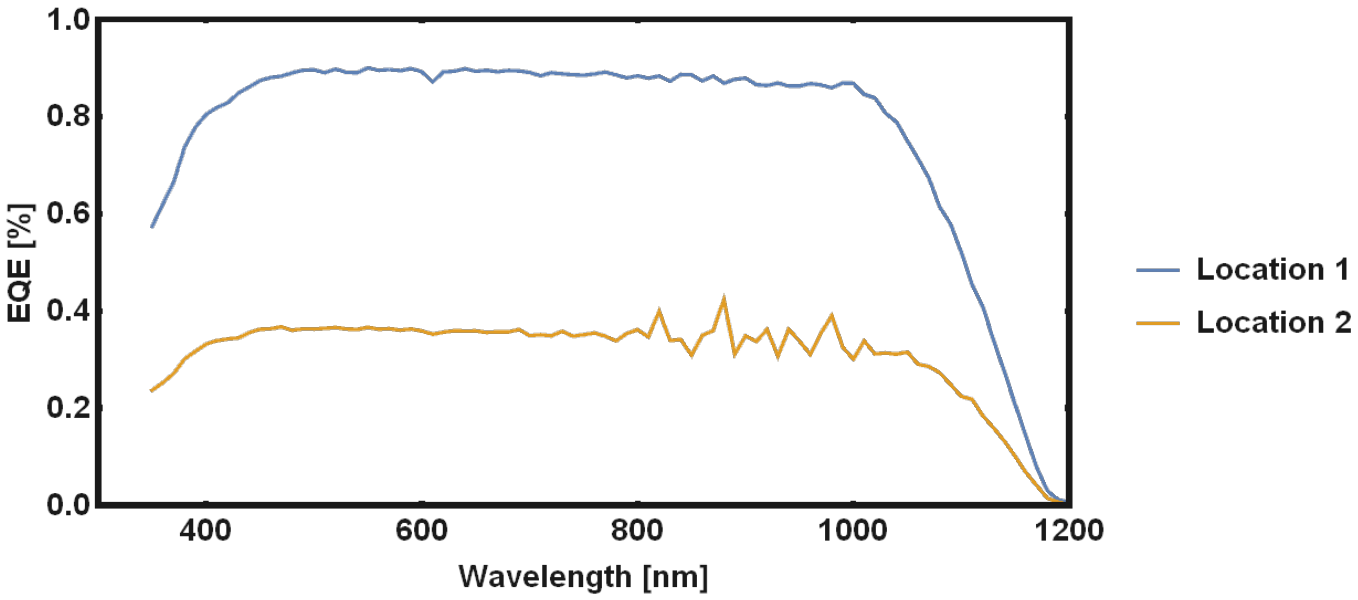

Figure 4.12: Quantum efficiency measurement on two different locations on the same HIT-IBC solar cell (15x45 mm). Location 2 is located slightly closer to the long edge of the device, whereas location 1 is located in the middle.

5 | Conclusions and Outlook

5.1 Conclusions

Today, silicon solar cells are dominating the photovoltaic market, with a market share of about 95%.[35] However, with silicon-based photovoltaics quickly approaching their efficiency limit of 29.4%,[5,6] other strategies to improve photovoltaic power conversion efficiency need to be explored. It has been shown recently that singlet fission enhanced silicon solar cells are a promising candidate to exceed conventional efficiency limits, with a potential to increase the efficiency of conventional silicon solar cells by 4.2% absolute.[27]

The main challenge that needs to be solved in utilizing the potential of singlet fission enhanced solar cells, is the challenge of transferring the energy from singlet fission-generated triplets to a low band-gap semiconductor. In this thesis, we have aimed to experimentally demonstrate the existence of this energy transfer from the singlet fission material tetracene to the low-bandgap semiconductor silicon. To this extent, we have built a device consisting of a tetracene add-on layer and a base HIT-IBC silicon solar cell. Devices with different interlayers have been fabricated to get insight in the processes playing a role in energy transfer. We have performed J(V)-measurements, magnetic field-dependent photocurrent measurements and quantum efficiency measurements to determine the existence of energy transfer from tetracene to silicon and their origin.

We have measured J(V)-curves throughout the fabrication process in section 4.1. These measurements show significant loss in J_{sc} as a result the removal of the silicon nitride anti-reflection layer and therefore we ascribe this loss to less efficient light absorption. The V_{oc} decreases as well, which we attribute an increase in surface recombination, since the passivating layer was also removed. After the tetracene evaporation, J_{sc} decreased even further, which we attribute to parasitic absorption, indicating that potential energy transfer from tetracene to silicon is not efficient.

To determine whether there is a contribution from the tetracene excitons to the photocurrent we extract from the solar cell, we measured the photocurrent in a magnetic field up to 0.4 T in section 4.2. According to Johnson-Merrifield

theory, photocurrent originating from singlet energy transfer should react differently to this magnetic field than photocurrent from a triplet exciton contribution. Initially, devices showed a magnetic field effect corresponding to singlet energy transfer. Since two devices included exciton blocking interlayers, we conclude that this magnetic field effect arises from photon transfer from prompt fluorescence. After an aging time of 6 weeks, we remeasured the magnetic field effect, finding a curve corresponding to triplet energy transfer for the device with direct interface between tetracene and silicon. Since the devices with exciton blocking interlayers did not show this inversion, we conclude that photon transfer from phosphorescence or delayed fluorescence cannot be the explanation for this curve. Furthermore, an experiment with white light bias from a halogen lamp excluded the possibility of the charging effect or trap state filling being responsible for the triplet effect. Therefore, we conclude that triplet energy transfer takes place in the device with a direct interface between tetracene and silicon with random pyramid structure.

To determine the important factors facilitating triplet energy transfer after the aging time, we have measured magnetic field effects for devices that were aged under nitrogen atmosphere and in ambient conditions. We found that for the device that was aged in a nitrogen-filled glovebox, the inversion of the magnetic field effect did not take place, whereas it did for the device that was aged under ambient conditions. This indicates that oxygen plays an important role in the aging process. This was confirmed by measuring the magnetic field effect for a device where the encapsulation step during the device preparation process was omitted. Initially, this device showed singlet energy transfer similar to the encapsulated devices. However, the inversion from singlet to triplet energy transfer took place after five days for this device, as opposed to six weeks for encapsulated devices. From this, we conclude that the growth of native silicon oxide facilitates triplet energy transfer from tetracene to silicon in singlet fission silicon solar cells.

To quantify the contribution from the triplet energy transfer indicated by the results from section 4.2, we have measured the quantum efficiency of our devices showing triplet magnetic field effect in section 4.3. In the absorbing wavelength range of tetracene, the measurements showed a decrease in quantum efficiency, corresponding to the absorption spectrum of tetracene. Furthermore, when we compared devices before aging (showing singlet magnetic field effect) and after aging (showing triplet magnetic field effect), no significant increase was visible. Therefore, we conclude that the previously indicated triplet energy transfer happens with an efficiency less than 5%.

5.2 Outlook

The results of magnetic field-dependent photocurrent measurements on our devices are very promising, showing that transfer of triplet energy can in fact take place between tetracene and silicon. However, quantum efficiency measurements showed that the transfer efficiency must be very low. This transfer efficiency can be quantified using an extended model that is used to determine quantum yield in tetracene solar cells.[33,37] It is clear that the transfer efficiency needs to be increased in order for this device to have any applications, but a proof-of-principle for triplet energy transfer from tetracene to silicon has been provided by this work.

From the results of this work, it followed that the appearance of the magnetic field effect for triplet is induced by oxygen exposure. However, it is not yet known what exactly happens during this process and what the mechanism for the triplets being able to transfer into the silicon is. Since this knowledge is of great importance in the effort of breaking the Shockley-Queisser limit using singlet fission enhanced solar cells, we recommend future studies to look into the cause of the triplet energy transfer, for instance by studying surface properties, composition and morphology of the devices that show triplet energy transfer.

The triplet energy transfer process needs to be increased to realize the potential of singlet fission solar cells. To do this, we recommend future studies to investigate the role of surface passivation quality. During the device preparation process in this work, the silicon nitride passivating layer of the HIT-IBC cells was removed, resulting in lower performance partially due to poor surface passivation quality. Poor surface passivation namely leads to high surface recombination, which lowers the performance of solar cells. Since triplet excitons in tetracene need to transfer their energy into silicon at the interface, high surface recombination at the silicon surface might be the reason that no triplet energy transfer was observed in the initial measurements. All energy from triplet excitons that is transferred to create an electron-hole pair would namely be lost almost instantly due to surface recombination. Since the photons from the observed photon transfer can be absorbed deeper into the silicon, photon transfer would suffer less from bad surface passivation, explaining our initial measurements indicating singlet energy transfer via photons.

The observation of triplet energy transfer after a certain aging time of the devices, might also be explained by surface passivation quality. It might be the case that the growth of silicon oxide improves the passivation quality of the silicon surface, thereby preventing the immediate loss of all triplet energy at the interface. However, as we have seen from the results from the devices with exciton blocking interlayers, the native silicon oxide can not grow too thick, since the energy transfer mechanism involved in triplet energy transfer, that is

Dexter transfer, heavily depends on the distance between donor and acceptor. Therefore, we recommend future studies to examine singlet fission silicon solar cells with similar architectures as used in this work, with the addition of a very thin passivating layer at the tetracene-silicon interface. This passivating layer should reduce the surface recombination, not impeding Dexter transfer from tetracene to silicon at the same time. The impact of such a passivating layer could be very significant, as it would not only improve the triplet energy transfer efficiency, but also the performance of the silicon base cell.

The importance of such a thin passivating interlayer between silicon and tetracene has recently been shown.[37] The authors report HfN_xO_y interlayers as thin as 8 Å facilitating triplet energy transfer from tetracene to crystalline silicon singlet fission-sensitized silicon solar cells. The authors report a singlet fission enhanced solar cell with power conversion efficiency of 5.1%. More importantly, they show an increase in quantum efficiency in the absorption range of tetracene, originating from the singlet fission process with maximum combined yield of the fission process of 133%.

The proof-of-principle presented in this report is a new step in the goal of circumventing the Shockley-Queisser limit and improving power conversion efficiency using singlet fission materials. However, the question that has arised now is how to improve the transfer efficiency, for which we have given some suggestions. Important work in answering this question is already being done by synthetic chemists, searching for new singlet fission materials with convenient exciton energy levels and efficient absorption and transmission in the relevant wavelength ranges. Next to this, focus should be on optimized device engineering, in order to make energy transfer from singlet fission materials to silicon applicable. For this, a complete understanding of the energy transfer processes at the interface is necessary.

Bibliography

[1] United Nations Framework Convention on Climate Change. The paris agreement. https://unfccc.int/process-and-meetings/the-paris-agreement/the-paris-agreement. Accessed: 18-02-2019.

[2] J Doyne Farmer and François Lafond. How predictable is technological progress? *Research Policy*, 45(3):647–665, 2016.

[3] Harry Wirth and Karin Schneider. Recent facts about photovoltaics in germany. http://large.stanford.edu/courses/2016/ph240/kumar1/docs/fraunhofer-14oct16.pdf, 2015. Accessed:02-07-2019.

[4] William Shockley and Hans J Queisser. Detailed balance limit of efficiency of p-n junction solar cells. *Journal of Applied Physics*, 32(3):510–519, 1961.

[5] Armin Richter, Martin Hermle, and Stefan W Glunz. Reassessment of the limiting efficiency for crystalline silicon solar cells. *IEEE Journal of Photovoltaics*, 3(4):1184–1191, 2013.

[6] Kunta Yoshikawa, Hayato Kawasaki, Wataru Yoshida, Toru Irie, Katsunori Konishi, Kunihiro Nakano, Toshihiko Uto, Daisuke Adachi, Masanori Kanematsu, Hisashi Uzu, et al. Silicon heterojunction solar cell with interdigitated back contacts for a photoconversion efficiency over 26%. *Nature Energy*, 2(5):17032, 2017.

[7] Albert Polman, Mark Knight, Erik C Garnett, Bruno Ehrler, and Wim C Sinke. Photovoltaic materials: Present efficiencies and future challenges. *Science*, 352(6283):aad4424, 2016.

[8] Octavi Escala Semonin. *Multiple Exciton Generation in Quantum Dot Solar Cells*. PhD thesis, University of Colorado, 2012.

[9] Antonio Luque and Antonio Martí. Increasing the efficiency of ideal solar cells by photon induced transitions at intermediate levels. *Physical Review Letters*, 78(26):5014, 1997.

[10] Bryan M Van Der Ende, Linda Aarts, and Andries Meijerink. Lanthanide ions as spectral converters for solar cells. *Physical Chemistry Chemical Physics*, 11(47):11081–11095, 2009.

[11] J De Wild, A Meijerink, JK Rath, WGJHM Van Sark, and REI Schropp. Upconverter solar cells: materials and applications. *Energy & Environmental Science*, 4(12):4835–4848, 2011.

[12] Dirk König, K Casalenuovo, Y Takeda, G Conibeer, JF Guillemoles, R Patterson, LM Huang, and MA Green. Hot carrier solar cells: Principles, materials and design. *Physica E: Low-dimensional Systems and Nanostructures*, 42(10):2862–2866, 2010.

[13] Michael Ettenberg and Henry Kressel. Solar cell device having two heterojunctions, November 2 1976. US Patent 3,990,101.

[14] Alexis De Vos. Detailed balance limit of the efficiency of tandem solar cells. *Journal of Physics D: Applied Physics*, 13(5):839, 1980.

[15] NREL. Nrel research efficiency chart. https://www.nrel.gov/pv/cell-efficiency.html. Accessed: 26-06-2019.

[16] Miha Filipič, Philipp Löper, Bjoern Niesen, Stefaan De Wolf, Janez Krč, Christophe Ballif, and Marko Topič. Ch 3 nh 3 pbi 3 perovskite/silicon tandem solar cells: characterization based optical simulations. *Optics Express*, 23(7):A263–A278, 2015.

[17] Moritz H Futscher and Bruno Ehrler. Efficiency limit of perovskite/si tandem solar cells. *ACS Energy Letters*, 1(4):863–868, 2016.

[18] MI Asghar, J Zhang, H Wang, and PD Lund. Device stability of perovskite solar cells–a review. *Renewable and Sustainable Energy Reviews*, 77:131–146, 2017.

[19] Martin A Green, Anita Ho-Baillie, and Henry J Snaith. The emergence of perovskite solar cells. *Nature Photonics*, 8(7):506, 2014.

[20] Millicent B Smith and Josef Michl. Singlet fission. *Chemical Reviews*, 110(11):6891–6936, 2010.

[21] Ching W Tang. Two-layer organic photovoltaic cell. *Applied Physics Letters*, 48(2):183–185, 1986.

[22] Charles L Braun. Electric field assisted dissociation of charge transfer states as a mechanism of photocarrier production. *The Journal of Chemical Physics*, 80(9):4157–4161, 1984.

[23] Daniel N Congreve, Jiye Lee, Nicholas J Thompson, Eric Hontz, Shane R Yost, Philip D Reusswig, Matthias E Bahlke, Sebastian Reineke, Troy Van Voorhis, and Marc A Baldo. External quantum efficiency above 100% in a singlet-exciton-fission–based organic photovoltaic cell. *Science*, 340(6130):334–337, 2013.

[24] Justin C Johnson, Arthur J Nozik, and Josef Michl. High triplet yield from singlet fission in a thin film of 1, 3-diphenylisobenzofuran. *Journal of the American Chemical Society*, 132(46):16302–16303, 2010.

[25] Johannes Zirzlmeier, Dan Lehnherr, Pedro B Coto, Erin T Chernick, Rubén Casillas, Bettina S Basel, Michael Thoss, Rik R Tykwinski, and Dirk M Guldi. Singlet fission in pentacene dimers. *Proceedings of the National Academy of Sciences*, 112(17):5325–5330, 2015.

[26] Millicent B Smith and Josef Michl. Recent advances in singlet fission. *Annual Review of Physical Chemistry*, 64:361–386, 2013.

[27] Moritz H Futscher, Akshay Rao, and Bruno Ehrler. The potential of singlet fission photon multipliers as an alternative to silicon-based tandem solar cells. *ACS Energy Letters*, 3(10):2587–2592, 2018.

[28] Mark WB Wilson, Akshay Rao, Bruno Ehrler, and Richard H Friend. Singlet exciton fission in polycrystalline pentacene: from photophysics toward devices. *Accounts of Chemical Research*, 46(6):1330–1338, 2013.

[29] L Jan Anton Koster, Sean E Shaheen, and Jan C Hummelen. Pathways to a new efficiency regime for organic solar cells. *Advanced Energy Materials*, 2(10):1246–1253, 2012.

[30] Seunghyup Yoo, Benoit Domercq, and Bernard Kippelen. Efficient thin-film organic solar cells based on pentacene/c 60 heterojunctions. *Applied Physics Letters*, 85(22):5427–5429, 2004.

[31] Jiye Lee, Priya Jadhav, and MA Baldo. High efficiency organic multilayer photodetectors based on singlet exciton fission. *Applied Physics Letters*, 95(3):192, 2009.

[32] Bruno Ehrler, Mark WB Wilson, Akshay Rao, Richard H Friend, and Neil C Greenham. Singlet exciton fission-sensitized infrared quantum dot solar cells. *Nano Letters*, 12(2):1053–1057, 2012.

[33] Tony C Wu, Nicholas J Thompson, Daniel N Congreve, Eric Hontz, Shane R Yost, Troy Van Voorhis, and Marc A Baldo. Singlet fission efficiency in tetracene-based organic solar cells. *Applied Physics Letters*, 104(19):193901, 2014.

[34] Luis M Pazos-Outón, Ju Min Lee, Moritz H Futscher, Anton Kirch, Maxim Tabachnyk, Richard H Friend, and Bruno Ehrler. A silicon–singlet fission tandem solar cell exceeding 100% external quantum efficiency with high spectral stability. *ACS Energy Letters*, 2(2):476–480, 2017.

[35] ISE Fraunhofer Institute for Solar Energy Systems. Photovoltaics report. https://www.ise.fraunhofer.de/content/dam/ise/de/documents/publications/studies/Photovoltaics-Report.pdf. Accessed: 19-06-2019.

[36] Rowan W MacQueen, Martin Liebhaber, Jens Niederhausen, Mathias Mews, Clemens Gersmann, Sara Jäckle, Klaus Jäger, Murad JY Tayebjee, Timothy W Schmidt, Bernd Rech, et al. Crystalline silicon solar cells with tetracene interlayers: the path to silicon-singlet fission heterojunction devices. *Materials Horizons*, 5(6):1065–1075, 2018.

[37] Markus Einzinger, Tony Wu, Julia F. Kompalla, Hannah L. Smith, Collin F. Perkinson, Lea Nienhaus, Sarah Wieghold, Daniel N. Congreve, Antoine Kahn, Moundi G. Bawendi, and Marc A. Baldo. Sensitization of silicon by singlet exciton fission in tetracene. *Nature*, 571:90–94, 2019.

[38] Nicholas J Thompson, Mark WB Wilson, Daniel N Congreve, Patrick R Brown, Jennifer M Scherer, Thomas S Bischof, Mengfei Wu, Nadav Geva, Matthew Welborn, Troy Van Voorhis, et al. Energy harvesting of non-emissive triplet excitons in tetracene by emissive pbs nanocrystals. *Nature Materials*, 13(11):1039, 2014.

[39] Felix Strieth-Kalthoff, Michael J James, Michael Teders, Lena Pitzer, and Frank Glorius. Energy transfer catalysis mediated by visible light: principles, applications, directions. *Chemical Society Reviews*, 47(19):7190–7202, 2018.

[40] David L Dexter. A theory of sensitized luminescence in solids. *The Journal of Chemical Physics*, 21(5):836–850, 1953.

[41] Chemistry LibreTexts. Dexter energy transfer. https://chem.libretexts.org/Bookshelves/Physical_and_Theoretical_Chemistry_Textbook_Maps/Supplemental_Modules_(Physical_and_Theoretical_Chemistry)/Fundamentals/Dexter_Energy_Transfer. Accessed: 28-06-2019.

[42] Th Förster. Zwischenmolekulare energiewanderung und fluoreszenz. *Annalen der Physik*, 437(1-2):55–75, 1948.

[43] Stefan Wil Tabernig. Förster resonance energy transfer from pbs quantum dots to silicon: The missing link towards singlet fission solar cells. Master's thesis, Universiteit van Amsterdam, 2018.

[44] Chemistry LibreTexts. Fluorescence resonance energy transfer. https://chem.libretexts.org/Bookshelves/Physical_and_Theoretical_Chemistry_Textbook_Maps/Supplemental_Modules_(Physical_and_Theoretical_Chemistry)/Fundamentals/Fluorescence_Resonance_Energy_Transfer. Accessed: 28-06-2019.

[45] RC Johnson and RE Merrifield. Effects of magnetic fields on the mutual annihilation of triplet excitons in anthracene crystals. *Physical Review B*, 1(2):896, 1970.

[46] RG Kepler, JC Caris, P Avakian, and E Abramson. Triplet excitons and delayed fluorescence in anthracene crystals. *Physical Review Letters*, 10(9):400, 1963.

[47] RC Johnson, RE Merrifield, P Avakian, and RB Flippen. Effects of magnetic fields on the mutual annihilation of triplet excitons in molecular crystals. *Physical Review Letters*, 19(6):285, 1967.

[48] Vijay Kumar, KN Bhat, and Niti Nipun Sharma. Surface modification of textured silicon and its wetting behaviour. *Journal of Adhesion Science and Technology*, 29(4):308–318, 2015.

[49] I Bertoti. Characterization of nitride coatings by xps. *Surface and Coatings Technology*, 151:194–203, 2002.

[50] Christopher J Bardeen. The structure and dynamics of molecular excitons. *Annual Review of Physical Chemistry*, 65:127–148, 2014.

[51] Koen van den Hoven. Harnessing singlet exciton fission to enhance silicon solar cells through direct charge-transfer. Master's thesis, Universiteit van Amsterdam, 2018.